DOE/CS/34138-T1

EXPERIMENTS WITH STRUCTURAL CONCRETE BLOCKS WHICH DOUBLE AS SOLAR AIR HEATERS

Final Report

By
Peter R. Payne
James P. Brown

April 1979

Work Performed Under Contract No. FG04-77CS34138

Payne, Inc.
Annapolis, Maryland

U.S. Department of Energy

Solar Energy

DISCLAIMER

DISCLAIMER

Available from the National Technical Information Service, U. S. Department of Commerce, Springfield, Virginia 22161.

Price: Printed Copy A04
Microfiche A01

DOE/CS/34138-T1
Distribution Category UC-59c

FINAL REPORT

EXPERIMENTS WITH STRUCTURAL CONCRETE BLOCKS WHICH DOUBLE AS SOLAR AIR HEATERS

by

Peter R. Payne
James P. Brown

for

U.S. Department of Energy
P.O. Box 5400
Albuquerque, New Mexico 87115

Grant No. EG-77-G-04-4138

Payne Inc.
1933 Lincoln Drive • Annapolis, Md. 21401

TABLE OF CONTENTS

ABSTRACT

Because concrete is a low cost, low "energy content" material, and because many buildings have unobstructed south-facing walls, the concept of an air heating structural block was evolved. This report describes four configurations, two routinely available from concrete block manufacturers, and two specially designed. Test walls were evaluated heating ambient air in a single pass, so the temperature difference was low. With that reservation, there was little difference between any of the configurations, (one of the "special" designs was best) or between the blocks and conventional solar air heaters.

In addition to the work covered in this final report, a paper was presented at the 13th Intersociety Energy Conversion Engineering Conference. Also, six theoretical and analytical studies, listed as References 1 through 6 were carried out during the subject program.

INTRODUCTION

One way of achieving low cost solar heat collection is to adapt a conventional concrete block wall, as shown in Figure 1. Since the (south-facing) wall is generally required in any case, the premium for solar heating is attributable to the glazing and manifolding. Figure 2 shows a section of such a wall on test. It might be expected that its collection efficiency would suffer because of the small contact area between block passage and the internally flowing air would result in a large temperature differential (ΔT) between them.

A specially designed "conventional" block (Figure 3) can give some increase in contact area and also minimize glazing costs by incorporating integral "frames" in the cast part. But the alternative configuration of Figures 4 and 5 enables the air/solid surface contact area to be increased by an order of magnitude, and eliminates the thermal resistance of the block wall.

The large blocks of Figures 4 and 5 proved to be too heavy for a mason to lift. We therefore built a smaller "standard size" block, Figures 6-8, which weighs about the same as a conventional construction block. As shown, it was intended to epoxy these together, but studies by construction specialists have since led to the conclusion that conventional mortar joints should be used. This requires the overall dimensions of the block to be reduced slightly, and enables the glazing recess to be dispensed with.

Due to the large thermal inertia of such blocks, conventional (i.e. NBS, ASHRAE) evaluation methods cannot be employed to measure their effectiveness as solar collectors. It is one purpose of this report to introduce appropriate alternative methodologies, and to present the results obtained when the temperature differences between the heated air and the ambient air were small.

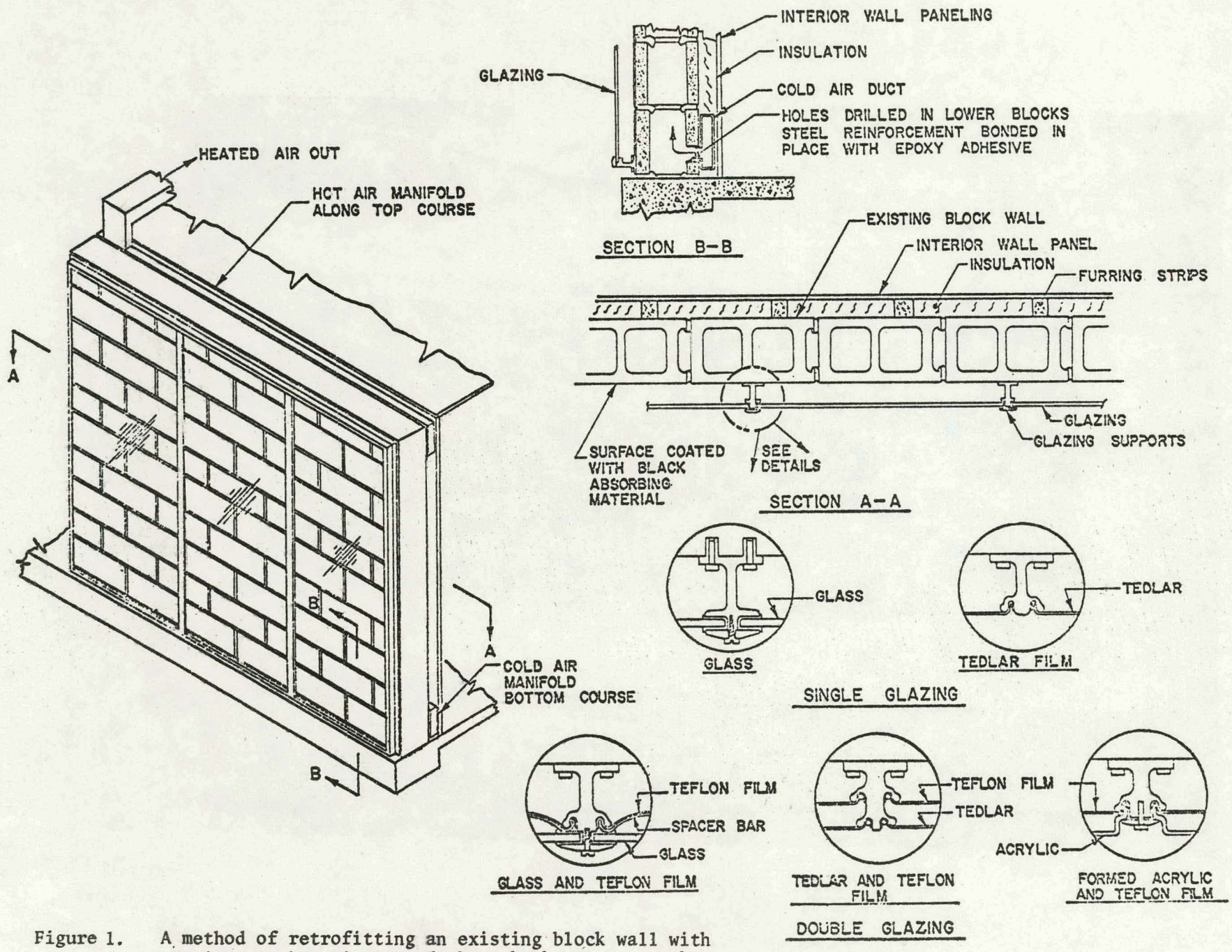

Figure 1. A method of retrofitting an existing block wall with glazing so that air passed through the cores can be heated.

Figure 2. A test section of a conventional block wall with simple glazing. In this photo the blocks have not yet received a selective coating.

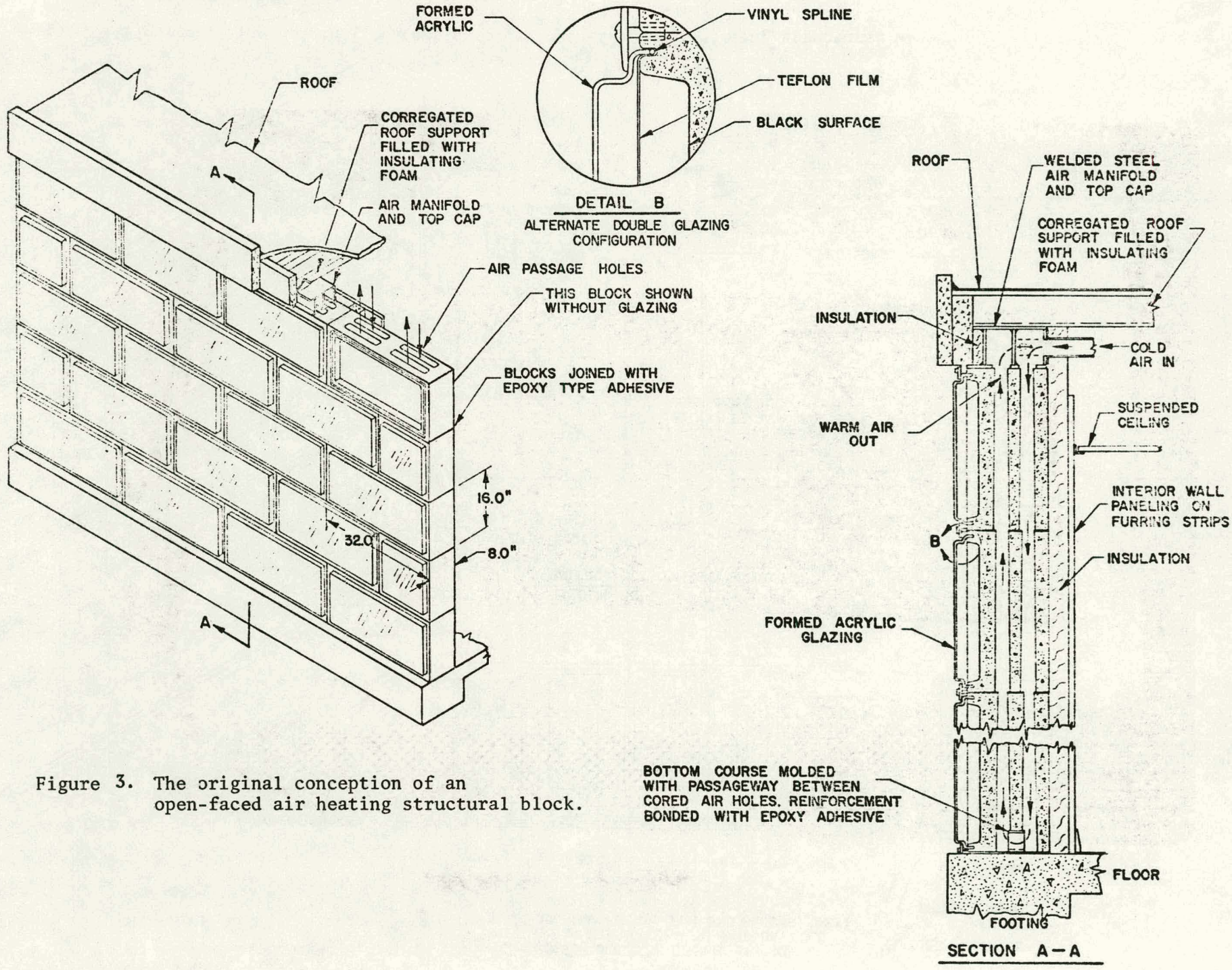

Figure 3. The original conception of an open-faced air heating structural block.

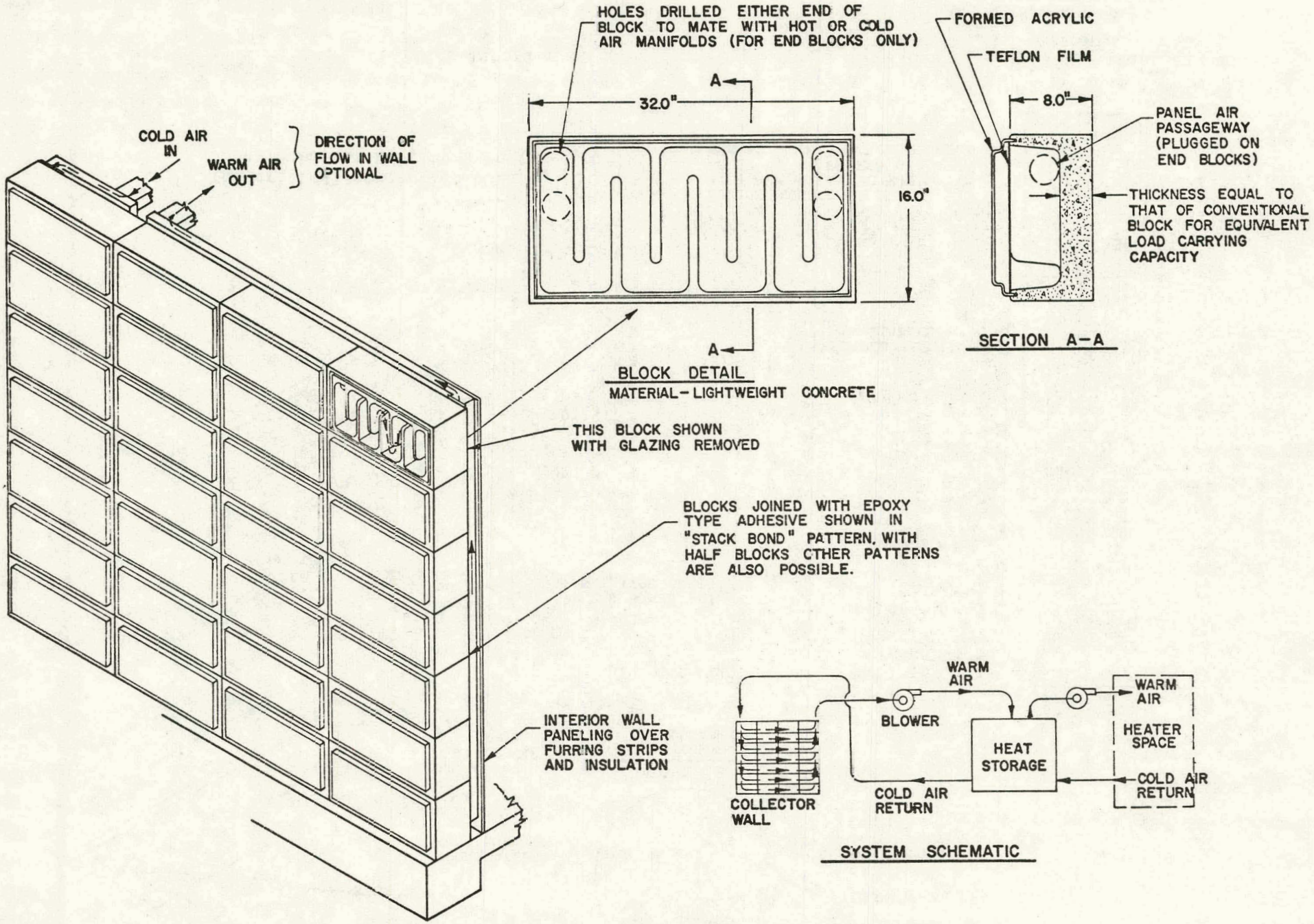

Figure 4. The original conception of an open-faced air heating structural block.

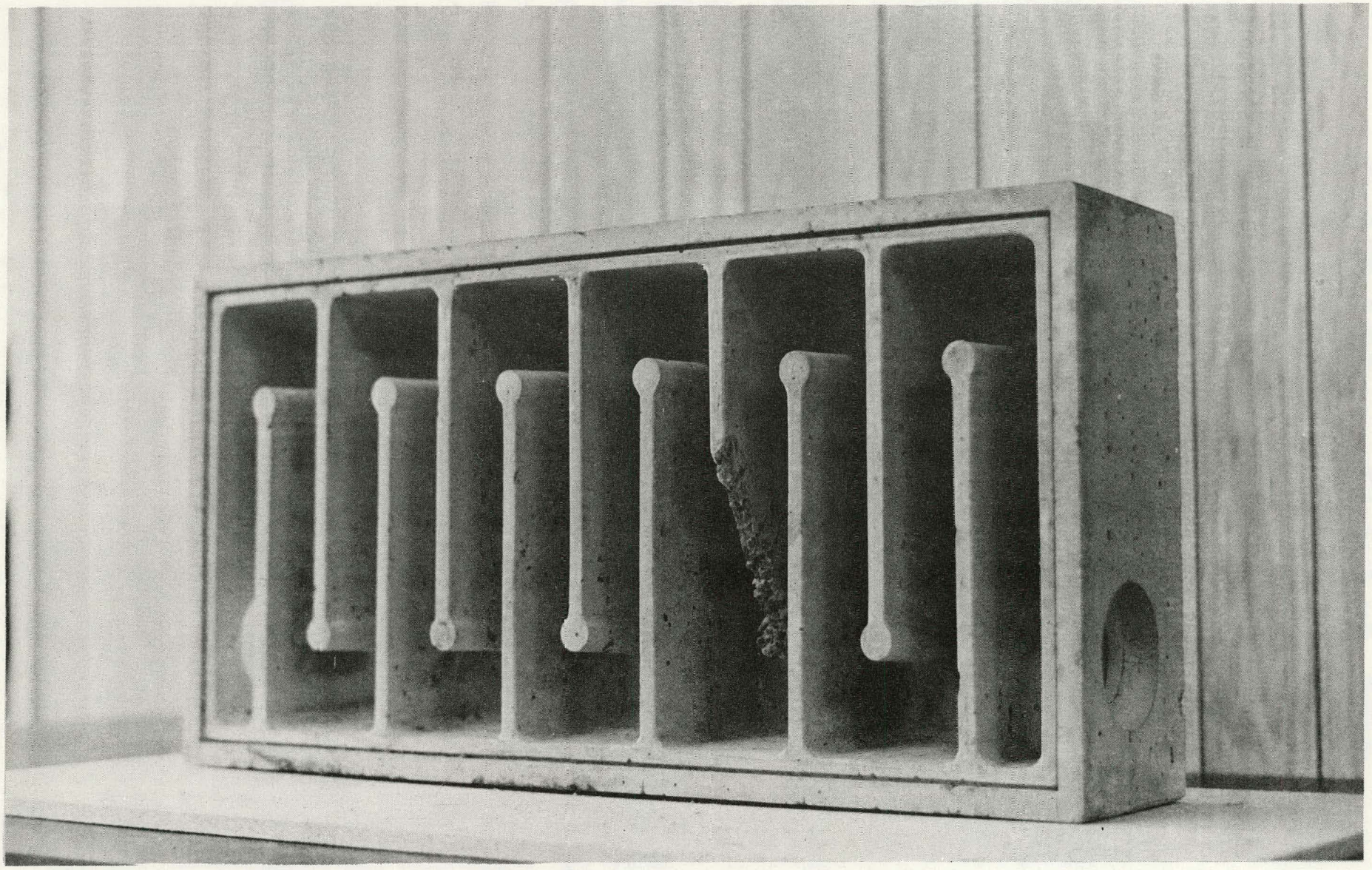

Figure 5. A large (8" × 16" × 32") open faced air heating block (as in Figure 22) cast from lightweight concrete. Air flows laterally from a port on the right vertical face to a corresponding one at the other end.

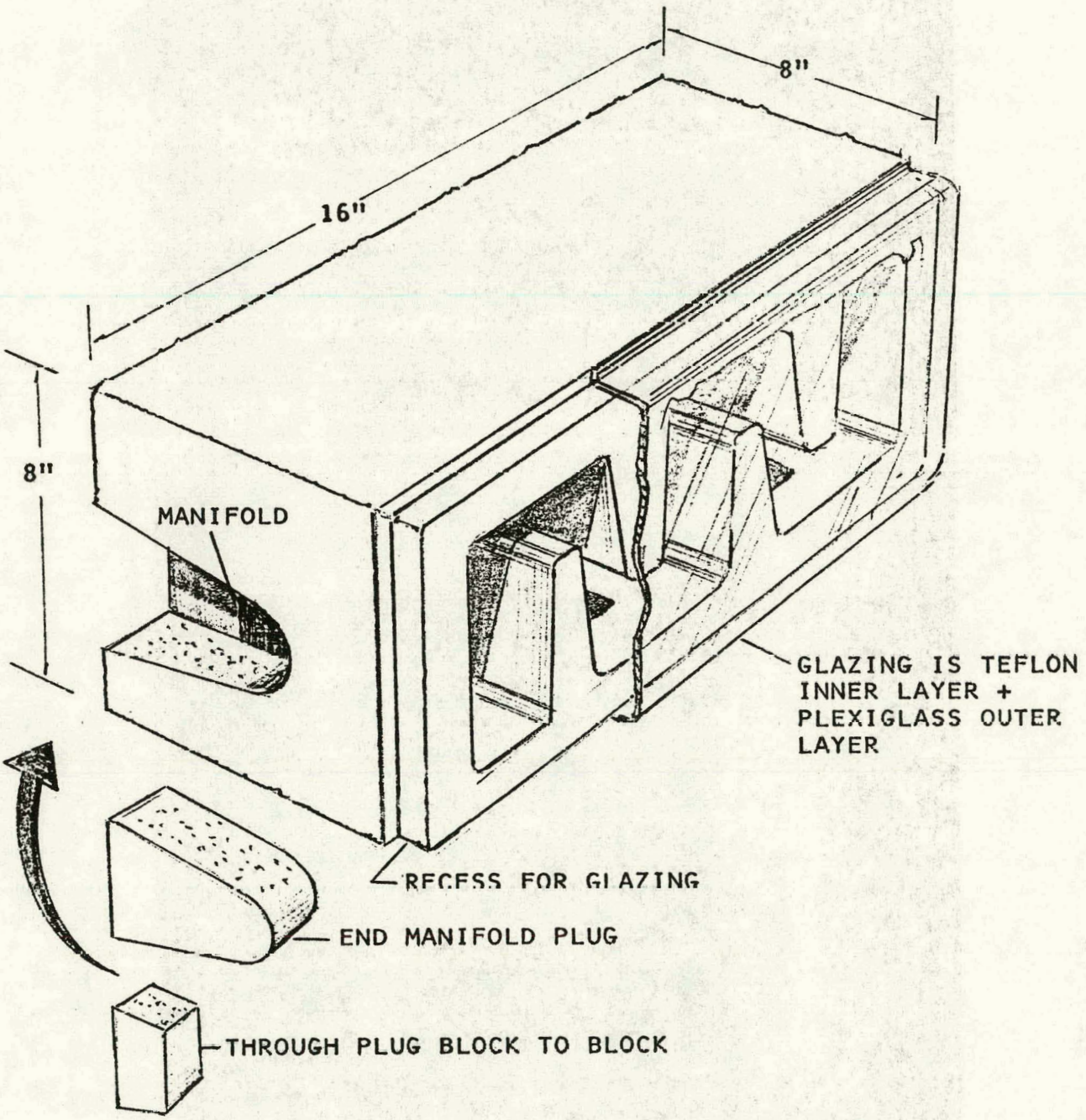

Figure 6. A standard size (8" x 8" x 16") concrete block.

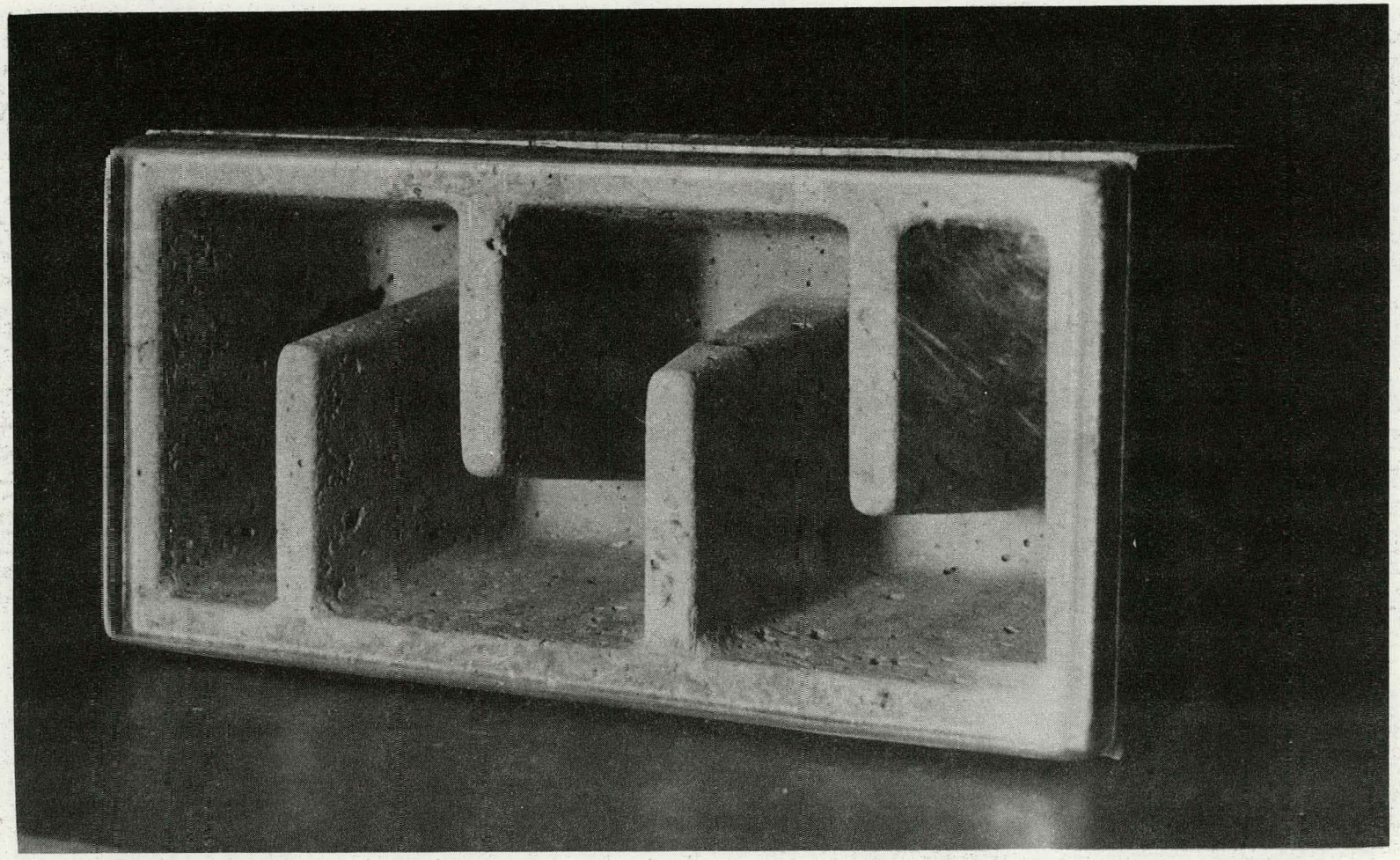

Figure 7. A prototype of the standard size open face block of Figure 22 and its outer glazing panel.

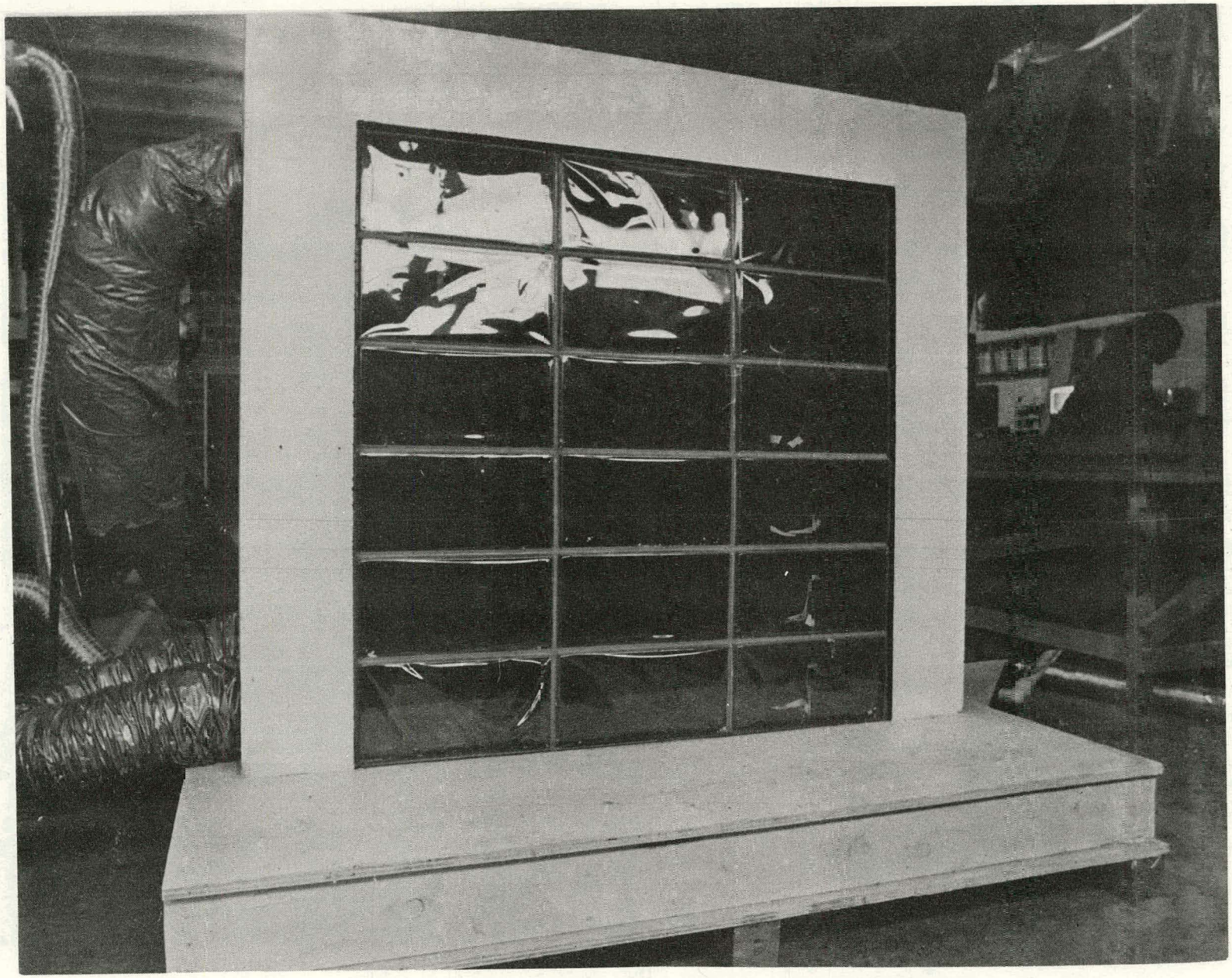

Figure 8. A test section wall of the open face block design in a "stack bond" configuration. The sides and back are insulated. Glazing is molded acrylic covers over Teflon film.

THEORETICAL BASIS

The basic method of measuring performance was to orient a test wall due south at the beginning of a day and pass air through it at a known rate and inlet temperature, measuring the outlet temperature and hence the heat gained. The thermal inertia of the test walls was typically of the order of 240 Btu/°F, or 15 Btu/ft^2°F, so that "equilibrium temperature" cannot be achieved because of the rate of change of insolation. On a clear day, the latter is approximately sinusoidal, i.e.

$$\Phi = \Phi_o \sin \Omega\theta$$

If

θ = time

T = average collector temperature

T_f = average throughput air temperature

T_∞ = ambient temperature

h = heat transfer coefficient

AK = heat loss coefficient of the insulation

a = (internal) heat transfer area

WC_p = thermal inertia

Then, if the collector efficiency is unity for simplicity, we have

$$\Phi_o \sin \Omega\theta = WC_p \frac{dT}{d\theta} + ah(T - T_f) + AK(T - T_\infty) \qquad (1)$$

(Insolation) = heat added to the block material + heat carried off by the working fluid + heat lost through the insulation

or

$$\frac{dT}{d\theta} + (\lambda_1 + \lambda_2)T = \mu \sin \Omega\theta + \lambda_1 T_f + \lambda_2 T_\infty \qquad (2)$$

where

$$\lambda_1 = ah/WC_p \qquad \lambda_2 = AK/WC_p \qquad \mu = \Phi_o/WC_p \qquad \Gamma = \lambda_1 + \lambda_2$$

The well-known solution for this first order linear equation is

$$T = e^{-\Gamma\theta}\left[\int e^{\Gamma\theta}\,(\mu \sin \Omega\theta + \lambda_1 T_f + \lambda_2 T_\infty)\, d\theta + C\right] \tag{3}$$

After some manipulation, this yields, for the collector temperature

$$T = \frac{\mu \sin(\Omega\theta + \phi)}{\sqrt{\Omega^2 + \Gamma^2}} + \frac{1}{\Gamma}(\lambda_1 T_f + \lambda_2 T_\infty)(1 - e^{-\Gamma\theta}) + [T_o + \mu\Omega/(\Omega^2 + \Gamma^2)]e^{-\Gamma\theta} \tag{4}$$

where the phase angle $\phi = \sin^{-1}(-\Omega/\sqrt{\Omega^2 + \Gamma^2})$

Equation (4) is plotted in Figure 9 for the following values:

$$\Phi_o = 193.0 \text{ Btu/ft}^2\text{hr}$$

$$ah = 52.93 \text{ Btu/°F.hr} \quad (\text{i.e. } h = 1 \text{ Btu/ft}^2\text{°F.hr})$$

$$AK = 29.03 \text{ Btu/°F.hr}$$

$$WC_p = 241.9 \text{ Btu/°F}$$

$$\Omega = 0.3173 \text{ hr}^{-1}$$

The phase angle is -0.7526 radians (-43.1°), but as shown in Figure 9, the peak block temperature occurs two hours after the maximum insolation.

For this reason, we elected to determine "all day" or "long period" efficiencies, defined as

$$\eta_{AIR} = \frac{\text{Heat transferred to the working fluid}}{\text{Total insolation on the vertical surface}}$$

and

$$\eta_{CUM} = \frac{\text{Heat transferred to the working fluid} + \text{Heat added to collector structure}}{\text{Total insolation on the vertical surface}}$$

There are, of course, other approaches. For example, one could assume a relationship for instantaneous efficiency, such as

$$\eta = \eta_o - \frac{\eta_1 (T - T_\infty)}{\Phi} \tag{5}$$

where

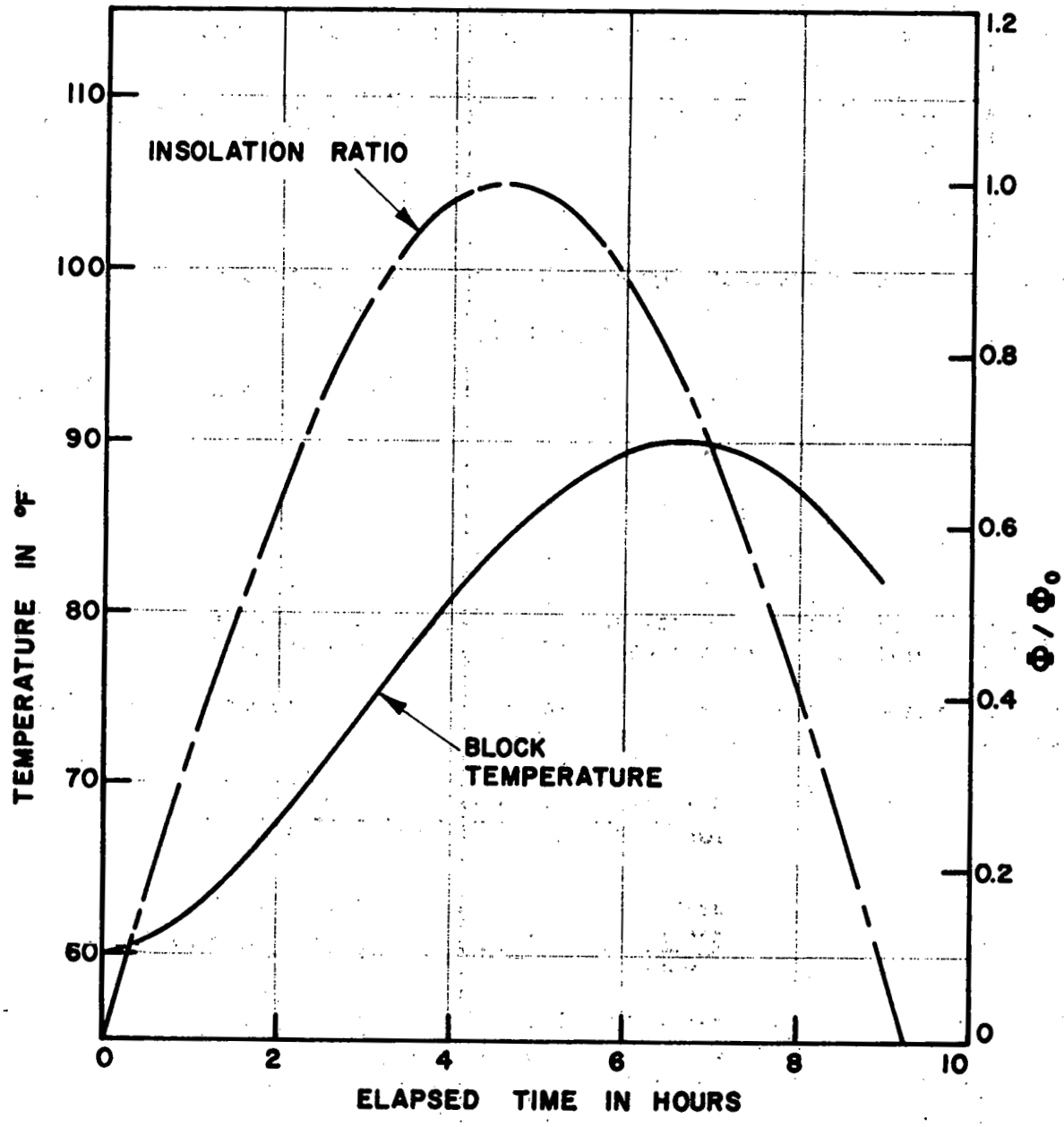

Figure 9. The theoretical variation of block temperature with time of day, from equation (4), using the values described in the text.

Φ = insolation

ΔT = temperature difference

η_o and η_1 are constants

Then one could conduct one's tests in such a way that the data can be made to yield values for the constants η_o and η_1.

The effect of incorporating equation (5) in equation (1) is instructive. This leads to

$$\frac{dT}{d\theta} + (\lambda_1 + \lambda_2 + \lambda_3)T = \mu\eta_o \sin \Omega\theta + \lambda_1 T_f + (\lambda_2 + \lambda_3)T_\infty \qquad (6)$$

where

$$\lambda_3 = \eta_1/WC_p$$

This is very similar to equation (2), but with the T and T_∞ coefficients modified.

Insolation was monitored with a Devices and Services Company Alphatometer mounted parallel to the wall surface. Inlet and outlet air temperatures were measured with a Natural Power Inc. digital differential thermometer. Typically, five thermocouple probes were mounted on the blocks; two at the back face, half an inch below the surface, and three on the middle of three vertical webs in the open part of the block, in the top, middle and bottom courses. The output of these thermocouples was read on a Love Corporation thermocouple meter.

Static pressure taps were used to measure the static pressure drop across the wall, in conjunction with a Dwyer inclined differential manometer. The air leaving the fan did so through a long, four-inch I.D. pipe and the mass flow through this was determined by a pitot-static traverse such as that shown in Figure 10. This is a normal type of "power law" distribution for the Reynolds number (Re 2.4×10^4) and from Schlichting[7] (pp. 563), we would expect a flow factor (average velocity divided by centerline velocity) of about 0.8 for an hydraulically smooth wall. The value actually measured from Figure 10 is 0.745, indicating some wall roughness.

The volume flow for the Figure 10 test is therefore

$$675 \times 0.745 \times \frac{\pi \times 4}{144} = 43.88 \text{ ft}^3/\text{min}$$

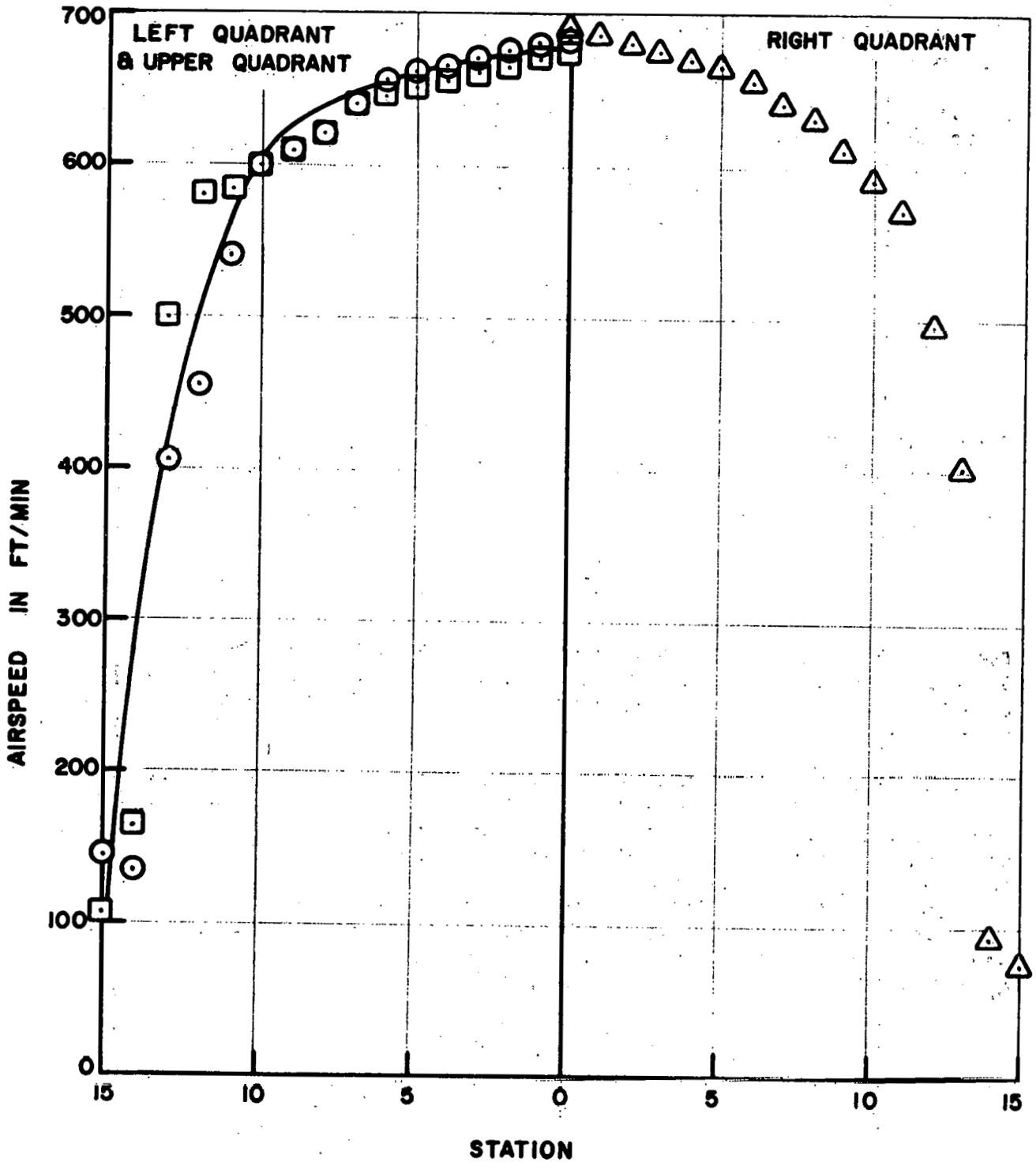

Figure 10. Velocity distribution in the exhaust duct.

The volume flow measurement given above was actually for the first test with the Payne open face blocks of Figures 6-8.

The pressure drop across the wall was 2.4 inches of water (12.48 lb/ft^2). The power loss associated with this is therefore

$$P = \text{pressure drop} \times \text{volume flow}$$

$$= 12.48 \times \frac{43.88}{60} = 9.127 \text{ ft.lb/sec}$$

$$= 42.23 \text{ Btu/hr}$$

$$= 12.38 \text{ watts}$$

$$= 0.0166 \text{ BHP}$$

Since the aperture of the wall is 16.3 ft^2, the additional 2.6 Btu/hr.ft^2 is negligible, even if we double it by assuming a fan efficiency of only 50%.

In terms of dynamic heads, the pressure drop coefficient is

$$\phi = \frac{12.48}{\frac{1}{2}\rho V^2} = \frac{12.48}{0.1505} = 82.9$$

There are 24 ports in the wall, and 4 x 18 = 72, 180° angle bends. If we assume $\phi = 0.9$ for each of the latter and $\phi = 1$ for each port we obtain, on the assumption that the flow velocity is unchanged, $\Sigma\phi = 87$. Thus the measured value makes sense.

To measure the heat lost through the insulation, the wall was connected to an air heater (Figure 11) in a closed circuit, in which all external insulated ducts were identical with those used when gathering heat from insolation. The glazing was insulated with two-inch polystyrene and six-inch fiberglass (equivalent to R29) during this experiment. The electrical load to the heater box was constant at 750 watts (2560 Btu/hr). Figures 12 and 13 give the air and block temperatures respectively during this test. Note from Figure 12 that the ΔT across the heater remained constant at 33.5 °C, throughout the test. Since $C_p \approx 0.241$ Btu/lb.°F for air, the weight flow must have been

$$\dot{W} = \frac{\dot{Q}}{C_p \Delta T} = \frac{2560}{0.841 \times 60.3} = 176.16 \text{ lb/hr}$$

$$= 2.936 \text{ lb/in}$$

$$\approx 38.4 \text{ ft}^3\text{/min}$$

which are not too different to the 43.9 ft^3/min measured during the insolation experiments. (There were, of course, additional flow pressure losses in the heating experiment.)

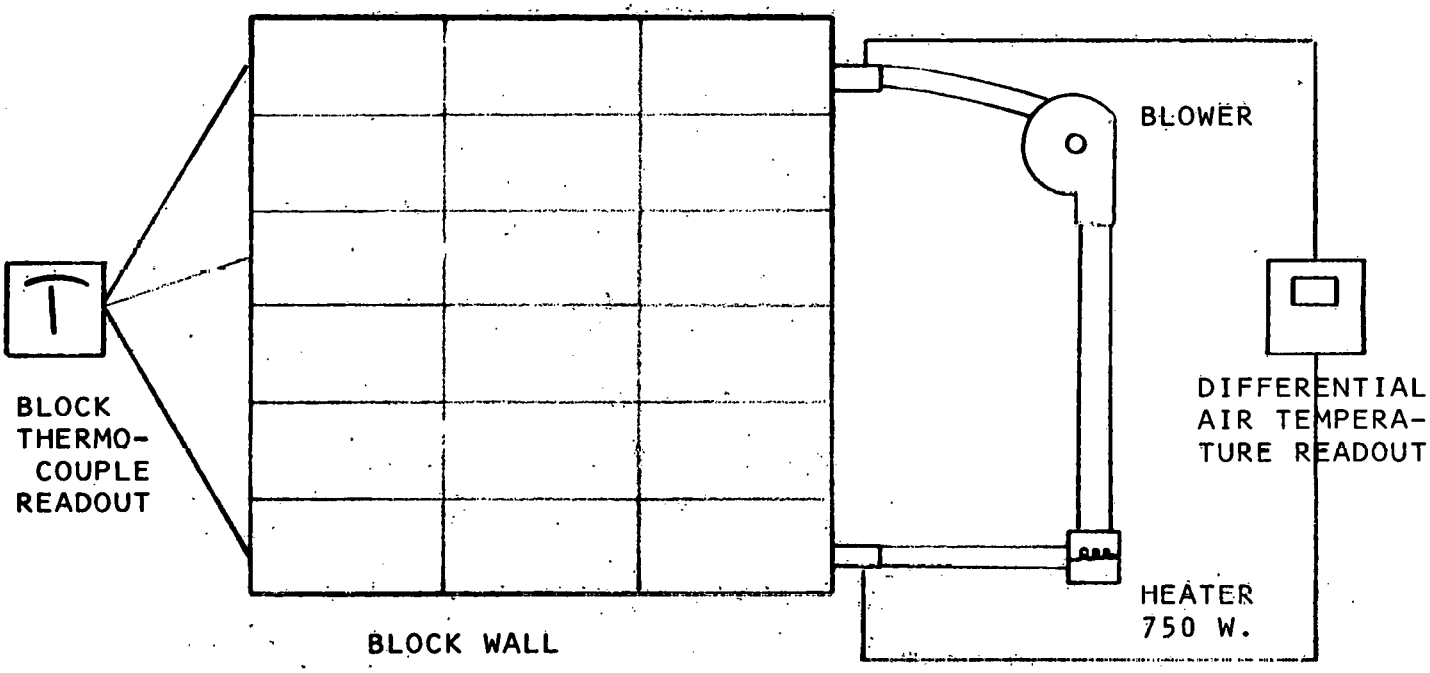

Figure 11. Schematic of insulation measurement experiments on solar heated concrete block wall.

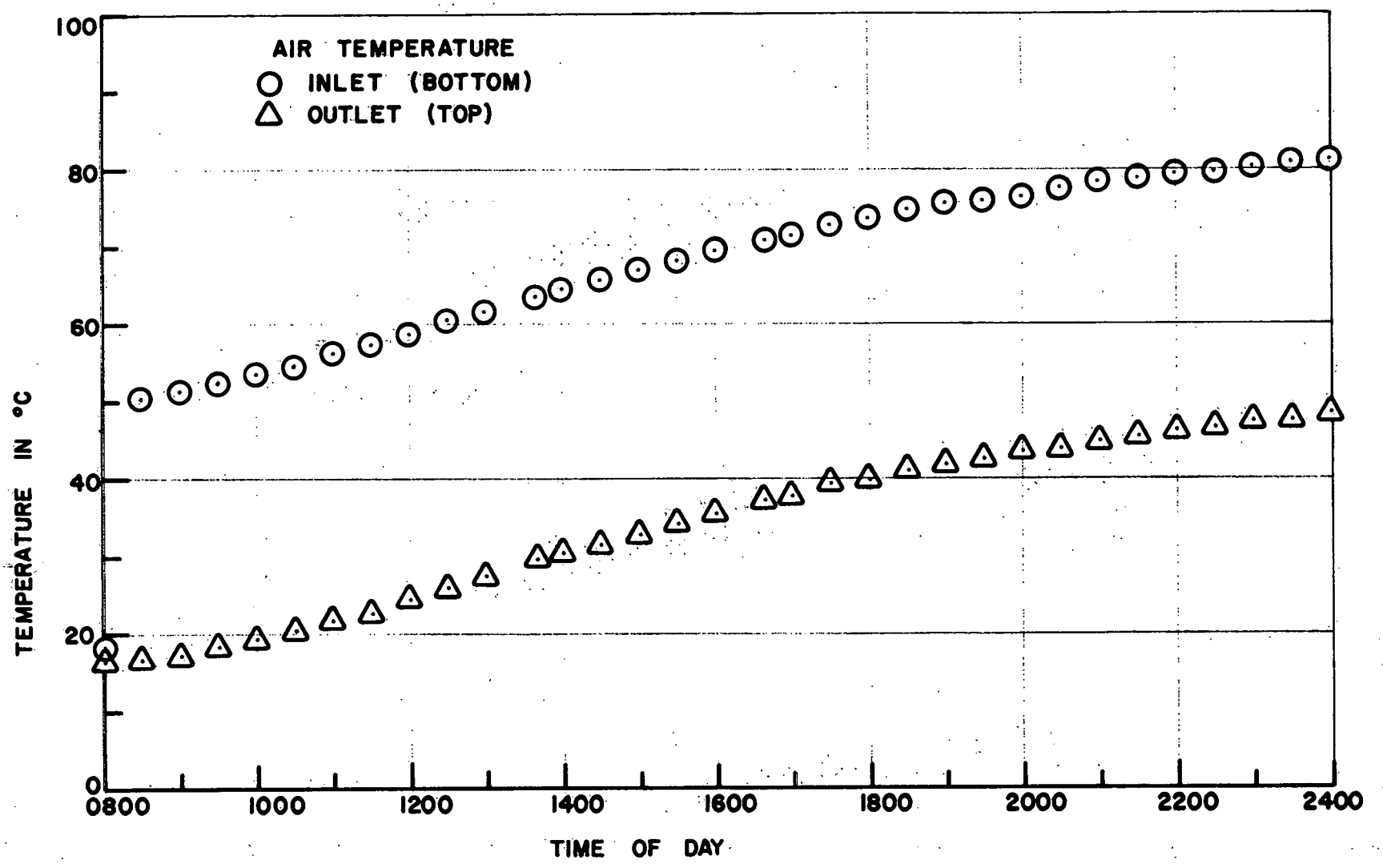

Figure 12. Air temperatures during closed circuit heating to determine insulation losses.

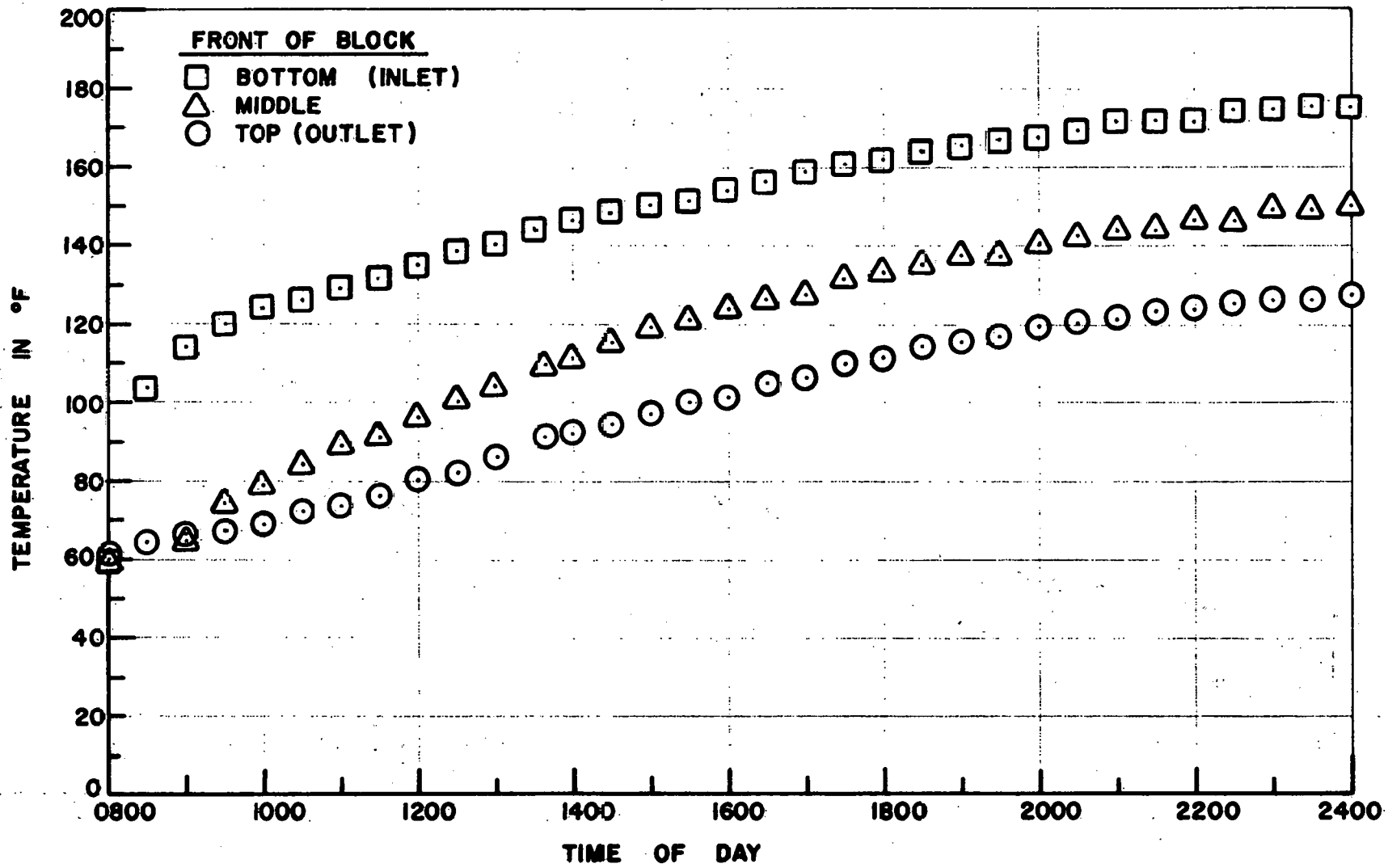

Figure 13(a). Front block temperatures during the closed circuit heating experiment.

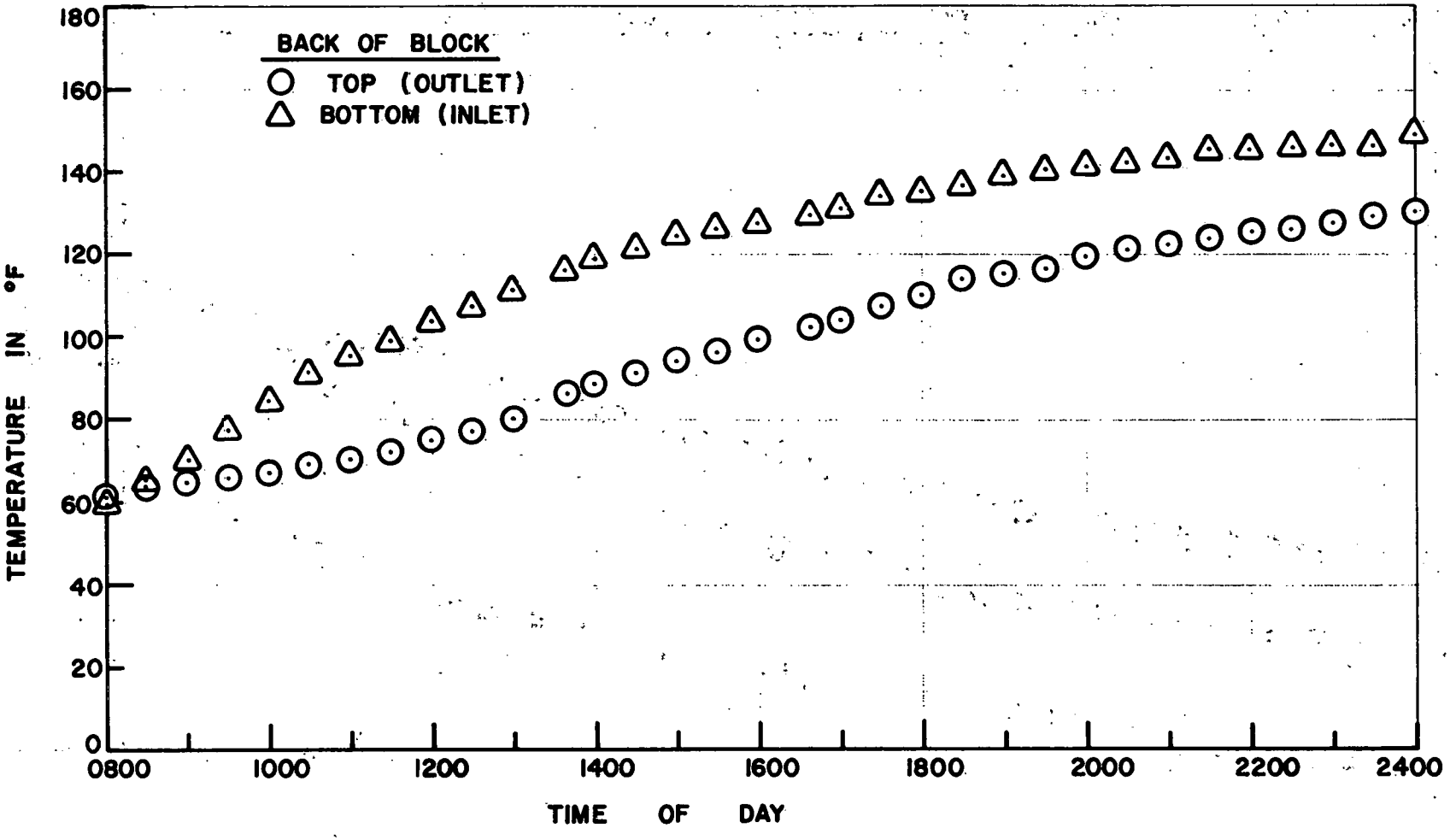

Figure 13(b). Rear block temperatures during the closed circuit heating experiments.

To determine the insulation value and thermal mass, we employed the following simple analysis, where the variables are the same as before. Let

$$q = \text{heat supply}$$

$$= WC_p \frac{dT}{d\theta} + AK(T - T_\infty) \tag{7}$$

$$\therefore \quad \frac{q}{WC_p} = \frac{dT}{d\theta} + \lambda_2(T - T_\infty) = z \tag{8}$$

where

$$\lambda_2 = AK/WC_p \text{ as before, and } z = q/WC_p$$

$$\therefore \quad \frac{dT}{d\theta} + \lambda_2 T = z + \lambda_2 T_\infty$$

$$\therefore \quad T = e^{-\lambda_2\theta}\left[\int e^{\lambda_2\theta}(z + \lambda_2 T_\infty)\, d\theta + C\right]$$

$$= \frac{z}{\lambda_2} + T_\infty + C\, e^{\lambda_2\theta}$$

when $\theta = 0$, $T = T_o$

$$\therefore \quad T = \frac{z}{\lambda_2} + T_\infty + (T_o - T_\infty - z/\lambda_2)e^{-\lambda_2\theta} \tag{9}$$

The maximum temperature is

$$T_M = z/\lambda_2 + T_\infty \tag{10}$$

so

$$T - T_M = (T_o - T_M)\, e^{-\lambda_2\theta}$$

$$\therefore \quad \lambda_2 = \frac{1}{\theta} \log[(T_M - T_o)/(T_M - T)] \tag{11}$$

Then

$$z = \lambda_2(T_M - T_\infty) \tag{12}$$

and

$$WC_p = q/z \tag{13}$$

$$AK = \lambda_2 WC_p \tag{14}$$

If the experiment is not carried out long enough to determine T_M, then λ_2 can be determined by a least mean squares curve fit of

$$A - Be^{-\lambda\theta}$$

to the data, where, from equation (9)

$$A = z/\lambda_2 + T_\infty$$

$$B = T_o - T_\infty - z/\lambda_2$$

This was done for the data of Figure 13, with the following results for $T_\infty = 70°$.

	Top Back	Bottom Back	Front Top	Middle Top	Bottom Top	Average
$A(=T_M°F)$	154	161	146	167	192	164
$B(°F)$	122.5	90.5	104.6	113.8	87.5	103.78
λ_2	0.102	0.124	0.110	0.119	0.105	0.112
$T_o(°F)$	31.5	70.5	41.4	53.2	104.5	60.22

The corresponding values of λ_2 for the inlet and exhaust air were 0.110 and 0.105, with T_M = 193.1 °F and 136.4 °F. In all cases, the "goodness of fit" was very high - of the order of 0.998 - but the initial temperatures are clearly much in error (although their average value is correct). This is presumed to be because the model (Equation 9) does not allow for the initial warm-up when the outer surfaces of the blocks have not yet changed their temperature. (In Figure 13, we see that the back of the front of the inlet block has risen 64°F in two hours whereas, in the same time, the back has only risen 24°F, a difference of 40 °F. This difference becomes less as the system stabilizes.) By eliminating these early readings from the curve fitting, we hope that errors due to this nonlinearity have been evaded to a large extent.

To compute the insulation loss, we take average values of

$$T_M = 164 \text{ °F}$$

$$\lambda_2 = 0.112$$

Also $$T_\infty = 22 \text{ °C} = 71.6 \text{ °F}$$

Thus

$$T_M - T_\infty = 92.4 \text{ °F}$$

$$z = \lambda_2(T_M - T_\infty) = 0.112 \times 92.4 = 10.35$$

$$WC_p = q/z = 2560/10.35 = 247.37 \text{ Btu/°F}$$

$$AK = \lambda_2 WC_p = 0.112 \times 247.37 = 27.71 \text{ Btu/hr.°F}$$

A convenient way of performing a sensitivity analysis is to repeat this calculation for the individual thermocouples, as shown in Table 1. The heat loss is least in the middle, as we would expect, and greatest at the top front. All the data looks reasonable. Maximum temperatures are highest near the hot air inlet and lowest near the exit.

The effective heat transfer coefficient (h) is obtained from the relationship

$$\frac{ah}{\dot{W}_a C_{p_a}} = \log [(T_{ao} - T_B)/(T_{ai} - T_B)] \qquad (15)$$

where

a is the internal surface area (52.92 ft^2)

T_{ai}, T_{ao} is the air temperature in and out

T_B is the mean block temperature

From the fitted curves

$$\frac{T_{ai} - T_B}{T_{ao} - T_B} = \frac{58.0 - 51.8\, e^{-0.105\theta} - 164 + 103.8\, e^{-0.112\theta}}{89.5 - 48.2\, e^{-0.11\theta} - 164 + 103.8\, e^{-0.112\theta}}$$

This is plotted in Figure 14, knowing that a = 52.92 ft^2, C_{p_a} = 0.241, $\dot{W}_a$ = 176.16 lb/hr. The values in Figure 14 look quite reasonable.

The test wall was exposed to insolation on May 3,* with results shown in Figures 15 - 17 and Table 2. The maximum temperature rise in the air (16.6°F) occurred at the end of the day's test, even though this was 3-1/2 hours after the maximum insolation.

It will be noted from Figure 16, that a drop in temperature occurred when a wind sprang up. This is probably due to an increased rate of heat transfer from the insulated box surrounding the wall, as well as additional heat loss from the glazing. If this is correct, then the "true" efficiency was somewhat higher than the values given in Figure 17. Another unknown source of error is the insolation absorbed by the white insolation case. Gebhardt[2] quotes 0.12 as the solar radiation absorbtivity of white lacquer. The areas involved as 7.70 ft^2 on the front, 8.125 ft^2 on the top and 7.17 ft^2 on each side. So, when one side and the top are illuminated, the total area is 23 ft^2. But 23 x 0.12 = 2.76 ft^2 or about 17% of the test aperture.

---

* Coincidentally, National SUN DAY

Table 1. Sensitivity Analysis

	Top Back	Bottom Back	Top Front	Middle Front	Bottom Front	Average
λ_2	0.102	0.124	0.110	0.119	0.105	0.112
$T_u - T_\infty$ (°F)	82.4	89.4	74.4	95.4	120.4	92.4
z	8.405	11.09	8.18	11.35	12.64	10.35
WC_p (Btu/°F)	304.6	230.9	312.8	225.5	202.5	247.37
AK (Btu/hr.°F)	31.07	28.64	34.41	26.83	31.26	27.71

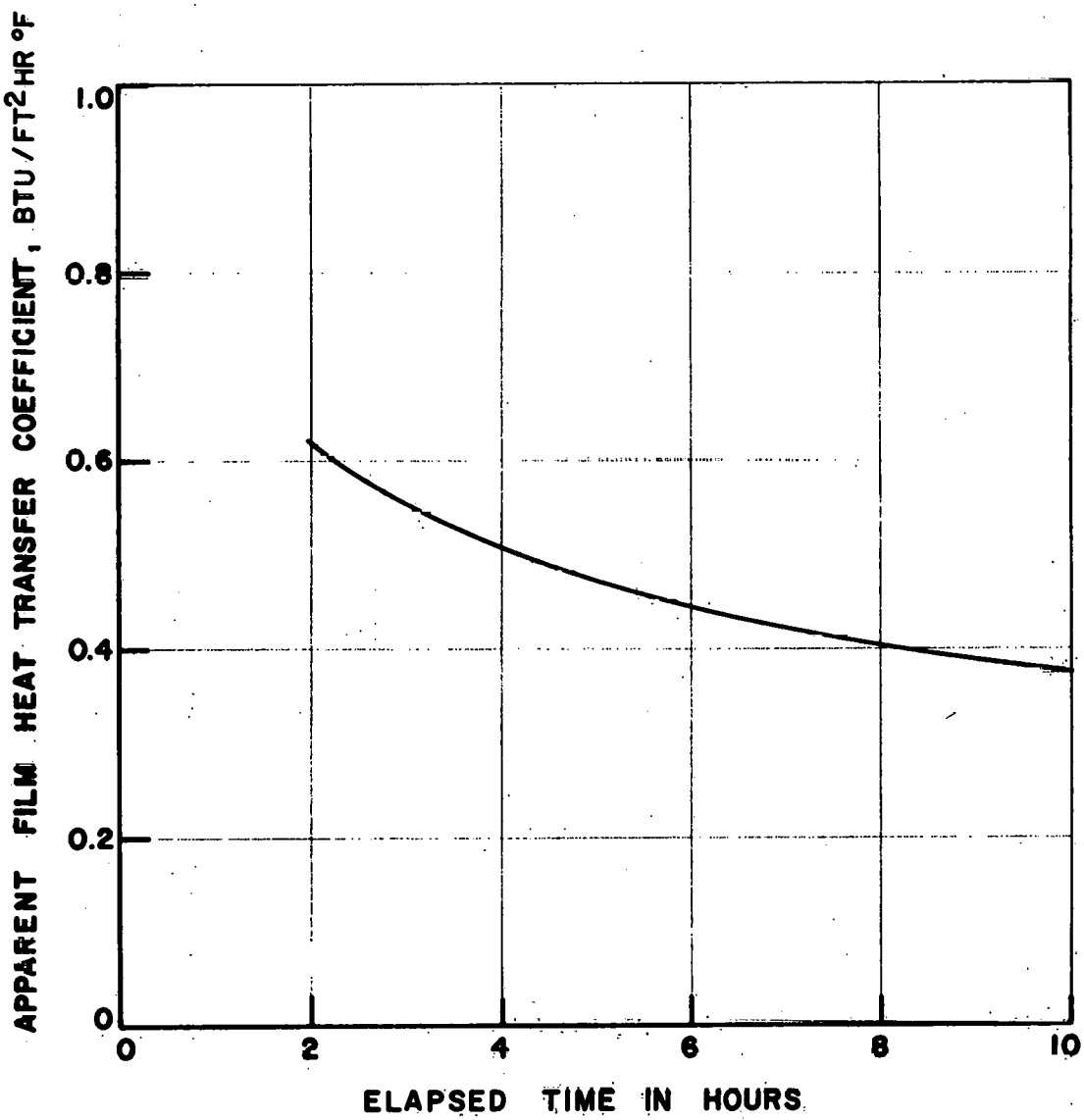

Figure 14. Variation of the apparent heat transfer coefficient with time during the insulation heating test.

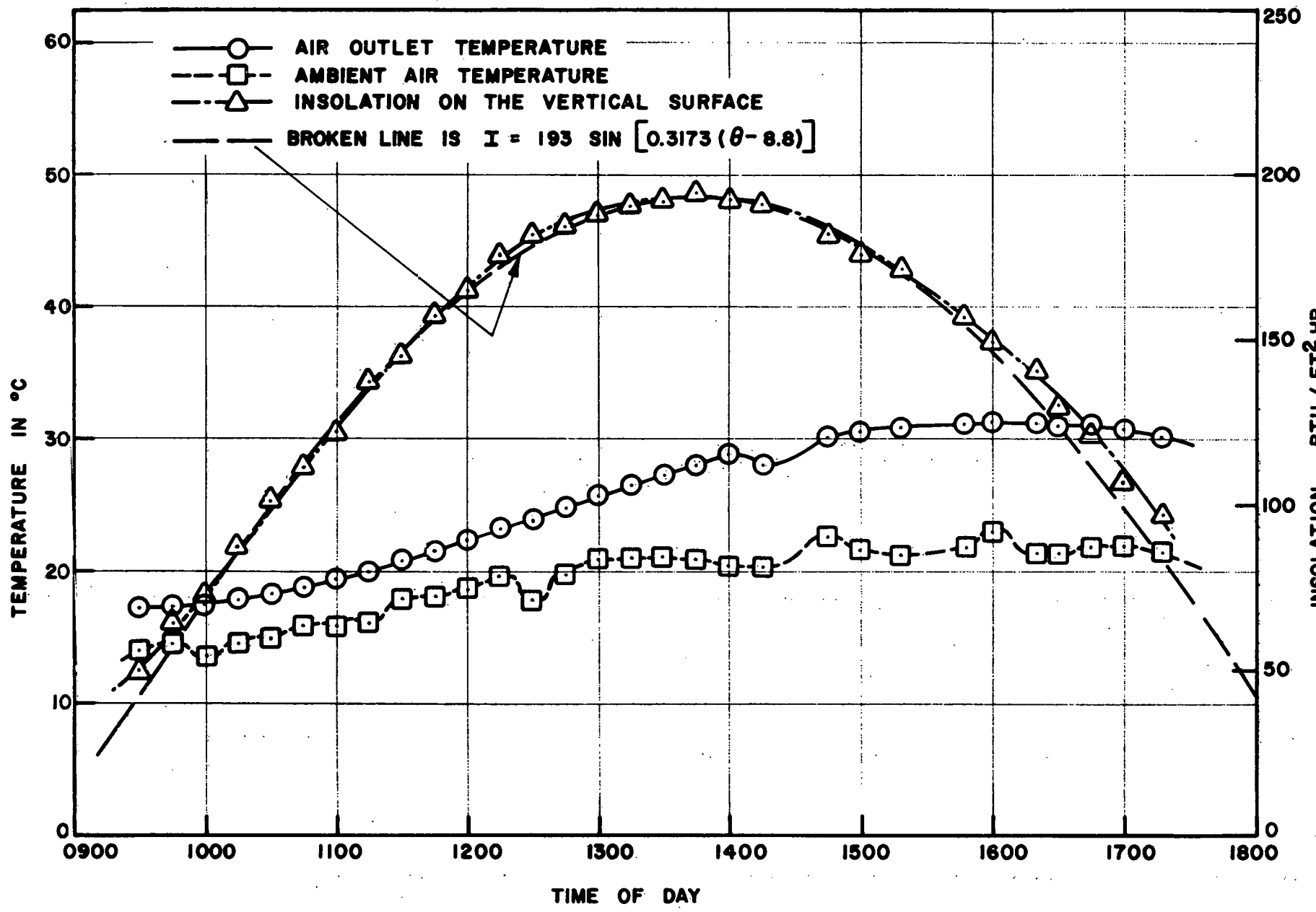

Figure 15. Standard size open face block wall performance on 3 May 1978. The ambient air was drawn into the wall and exhausted by a fan. Volume flow was 43.9 ft^3/min.

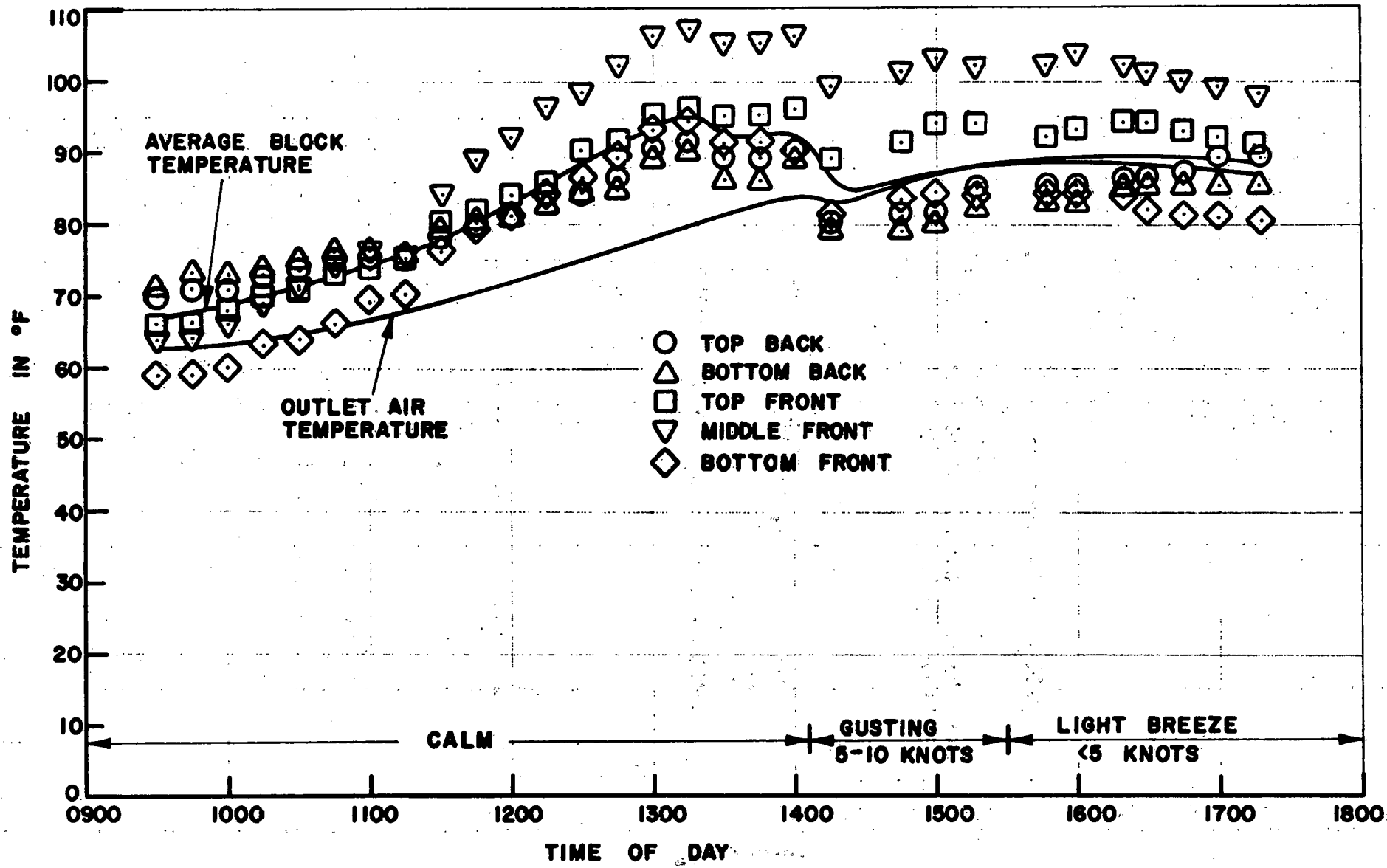

Figure 16. Block temperatures during the test on 3 May 1978.

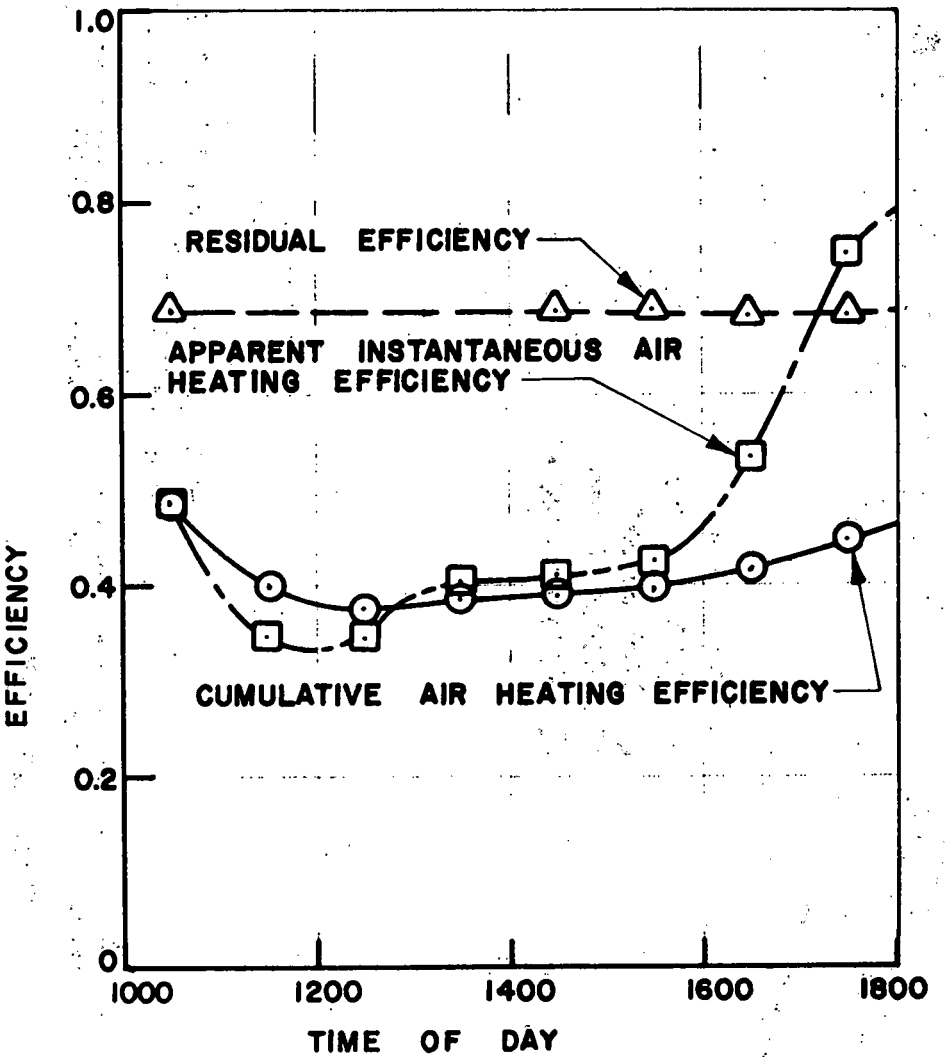

Figure 17. Efficiency of the open face block wall on 3 May 1978. Volume flow = 43.9 ft^3/min.

Table 2. Open face air block performance on 3 May 1978

	9:30-10:30	10:30-11:30	11:30-12:30	12:30-1:30	1:30-2:30	2:30-3:30	3:30-4:30	4:30-5:30
Average insolation (Btu/ft^{2}hr)	73	122	165	188	190	176	150	110
Average block temperature °F	69	74	83.3	93.5	90.0	87	89	89
Average ambient temperature °C	14.5	16.0	18.0	20.0	20.5	21.8	22.0	21.5
Average insulation heat loss (Btu/ft^2)	19.4	23.5	33.66	45.42	37.58	28.07	30.99	32.59
Average outlet temperature °C	17.5	19.4	22.3	25.6	28.0	30.4	31.1	30.7
ΔT °C	3.0	3.4	4.3	5.6	7.5	8.6	9.1	9.2
Heat collected by air (Btu)	262.5	297.5	376.2	490.0	656.2	752.5	796.2	805.0
Heat collected (Btu/ft^2)	16.10	18.25	23.08	30.06	40.25	46.16	48.84	49.38
Total Collection + insulation heat loss (Btu/ft^2)	35.5	41.76	56.74	75.48	77.83	74.23	79.83	81.97
Apparent efficiency	0.486	0.342	0.343	0.401	0.41	0.422	0.532	0.745
Cumulative insolation (Btu/ft^2)	73	195	360	548	738	914	1064	1174
Cumulative heat collected (Btu/ft^2)	35.5	77.26	134.0	209.48	287.31	361.54	441.37	523.34
Cumulative air heating efficiency	0.486	0.396	0.372	0.382	0.389	0.395	0.415	0.446

To test this effect, the surfaces previously painted white were covered with shiny aluminum foil. Also the case insulation was roughly doubled. The results of tests with this set up on June 12 are presented in Table 3 and Figures 18 - 20. The days end cumulative air heating efficiency is reduced from 44.6% to 35%. This could be due to the changes. On the other hand, it could be due to the higher winds experienced on June 12, and/or the fact that the sun was higher in the sky.

Other Configurations Tested

The large block illustrated in Figures 4 and 5 was tested by itself, with results given in Table 4 and Figures 21 - 23.

The cinder block wall of Figure 1 was tested in the same way as the open face design, with the results given in Table 5 and Figures 24 - 26. Surprisingly, it was not significantly inferior to open face design. This may not hold for higher temperature differences, however.

A final configuration, suggested by the Program Monitor, Dr. Donald Neeper, involved passing the air over the outside of a standard ornamental fluted block, between the block and the (single) glazing. As Table 6 and Figures 27 - 29 attest, the performance was comparable with the other configurations.

Table 3. Thermal performance of small Payne open face block on June 12, 1978

	10:30-11:30	11:30-12:30	12:30-1:30	1:30-2:30	2:30-3:30
Average insolation (Btu/ft^2hr)	129	151	156	146	120
Average block temperature °F	92	99	104	105	102
Average ambient temperature °C(°F)	23.9(75.0)	25.1(77.2)	26.2(79.2)	27.7(81.9)	28.1(82.6)
Average outlet temperature °C(°F)	26.2(79.2)	28.1(82.6)	30.1(86.2)	31.7(89.1)	32.0(89.6)
ΔT (air) °C(°F)	2.3(4.2)	3.0(5.4)	3.9(7.0)	4.0(7.2)	3.9(7.0)
Heat collected (air) (Btu/ft^2hr)	13.9	17.2	23.2	23.9	23.2
Average insulation loss (Btu/ft^2hr)	25.2	32.3	36.7	34.2	28.7
Total heat collected (Btu/ft^2hr) (corrected for blower)	36.3	46.7	57.1	55.3	49.1
Instant air efficiency	0.28	0.31	0.37	0.38	0.41
Cumulative insolation (Btu/ft^2)	129	280	436	582	702
Cumulative heat collected(Btu/ft^2)	36.3	83.0	140.1	195.4	244.5
Cumulative efficiency	0.28	0.30	0.32	0.34	0.35
Residual heat gain in block(Btu/ft^2hr)	140/7	123.1	84.4	0	0
Residual Efficiency	1.37	1.12	0.91	0.38	0.41

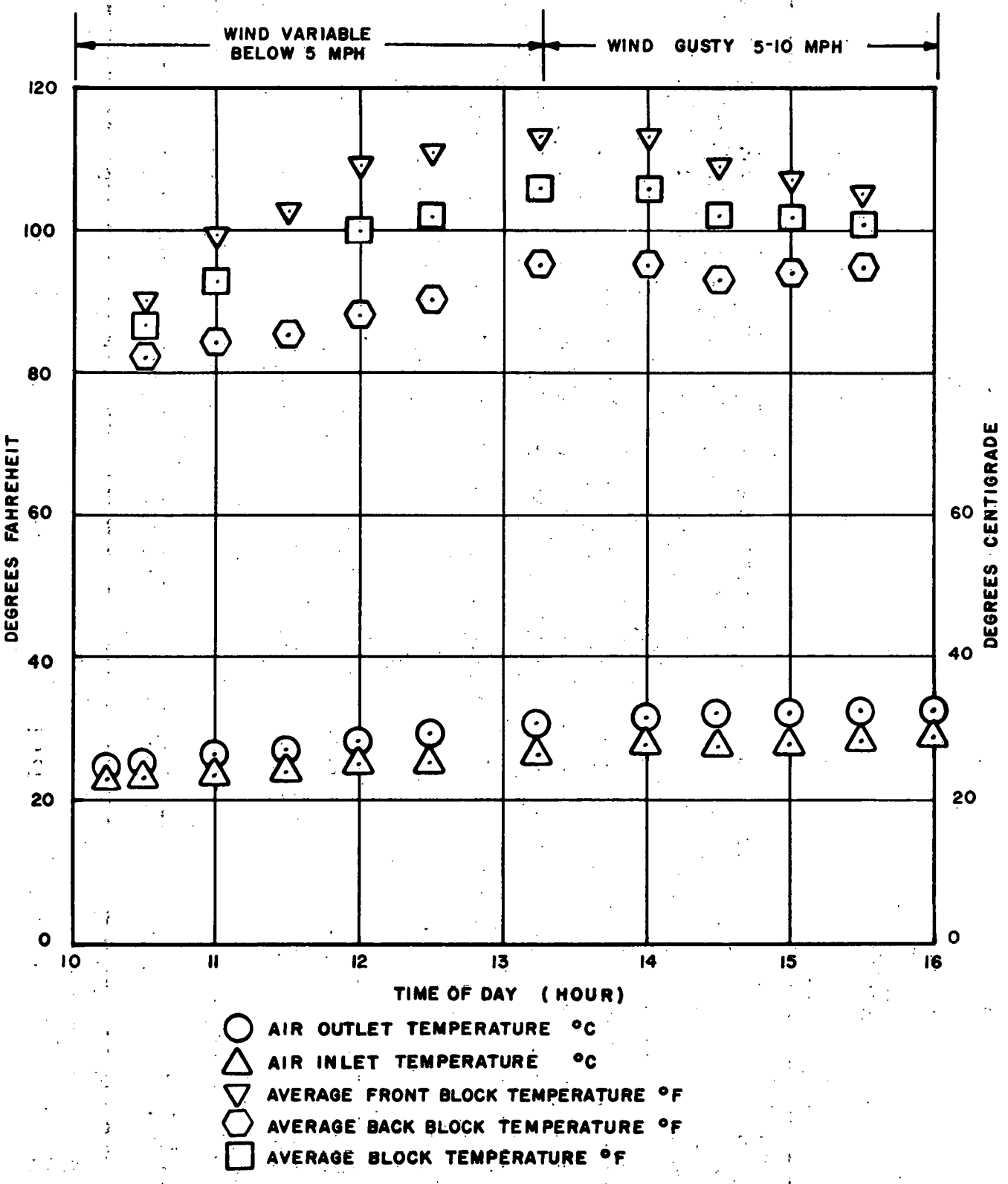

Figure 18. Air and block temperatures for the small Payne open face block test on 6/12/78.

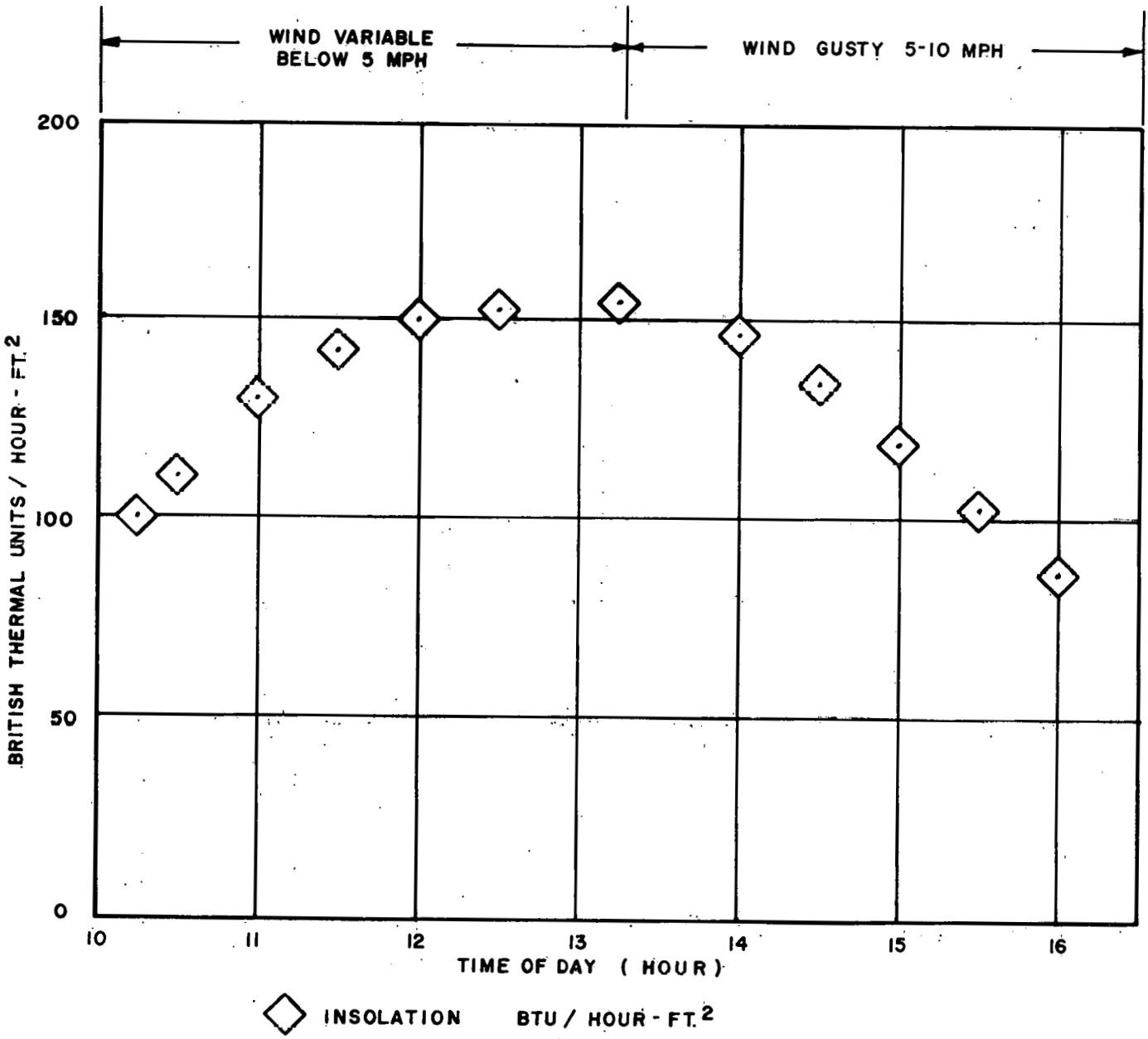

Figure 19. Insolation on the vertical wall during the small Payne open face block tests on 6/12/78.

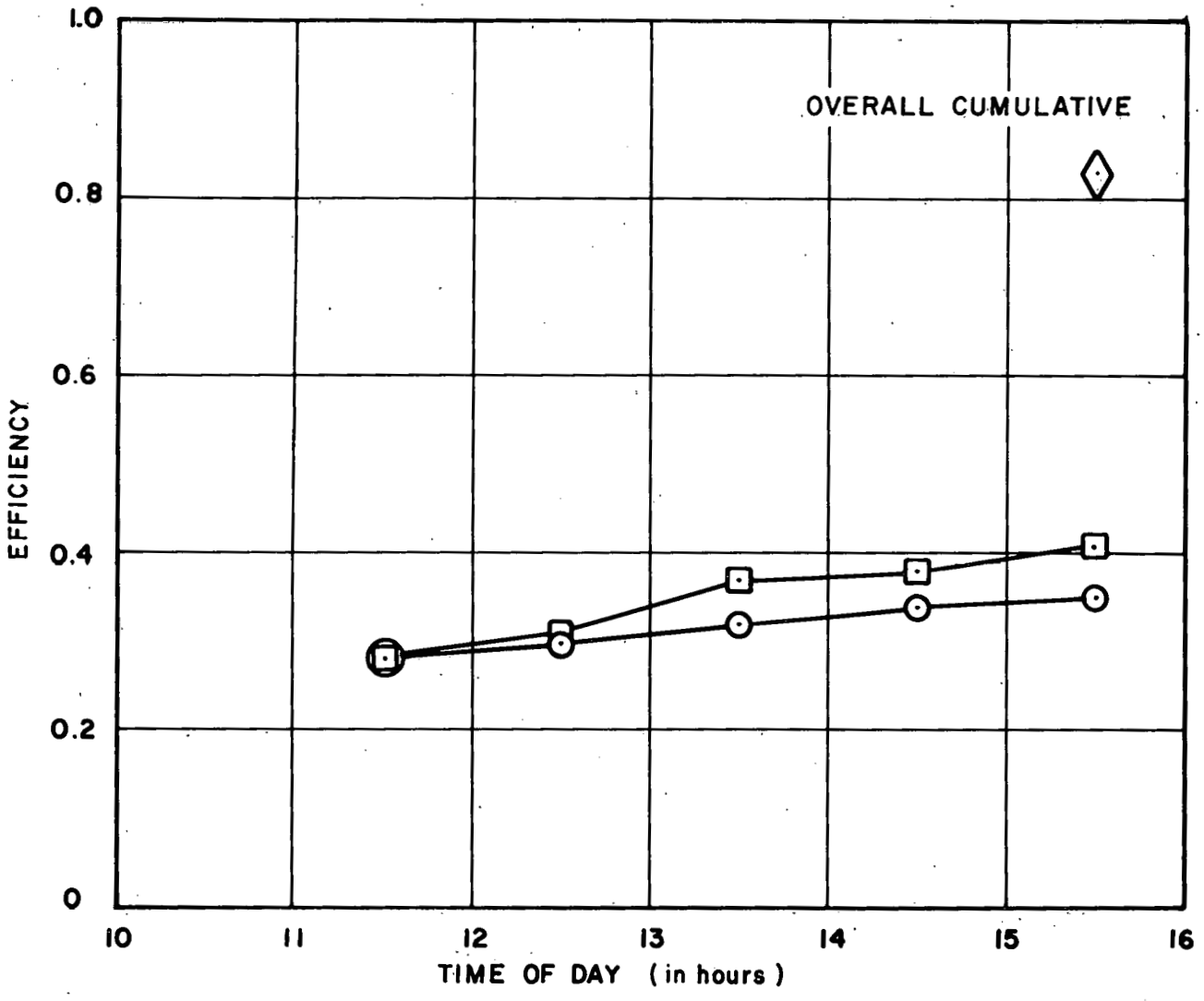

Figure 20. Efficiency of a small Payne open-face block wall, aperture 13.2 ft^2, vertical and south-facing, on 6/12/78 at Annapolis, MD. Double glazing of acrylic and polyester with air flow of 43.8 CFM. Block surface painted with Nextel black.
Pressure drop = 2.5 in. H_2O

Table 4. Thermal Performance, large Payne open face block

	10:00-11:00	11:00-12:00	12:00-1:00	1:00-2:00
Average insolation (Btu/ft^2hr)	267	284	283	288
Average block temperature °F	91.4	105.7	113.5	113.1
Average ambient temperature °C	27.7	30.9	32.5	33.4
Average outlet temperature °C	29.7	37.9	43.1	46.4
ΔT (air) °C	2.0	7.0	10.6	13.0
Heat collected (air) (Btu/ft^2hr)	25.4	88.7	134.4	164.8
Average insulation loss (Btu/ft^2hr)	13.1	24.8	31.5	28.8
Total heat collected (Btu/ft^2hr) corrected for blower (-.13Btu/ft^2hr)	38.4	113.4	165.8	193.4
Instant air efficiency	0.14	0.40	0.59	0.67
Cumulative insolation (Btu/ft^2hr)	267	551	834	1122
Cumulative heat collected (Btu/ft^2hr)	38.4	151.8	317.6	511.0
Cumulative efficiency	0.14	0.28	0.38	0.46
Residual heat gain in block (Btu/ft^2hr)	206.0	156.8	0.0	59.8
Total air and block heat/hr	244.4	270.2	165.8	253.2
Residual efficiency plus air instantaneous	0.92	0.95	0.59	0.88

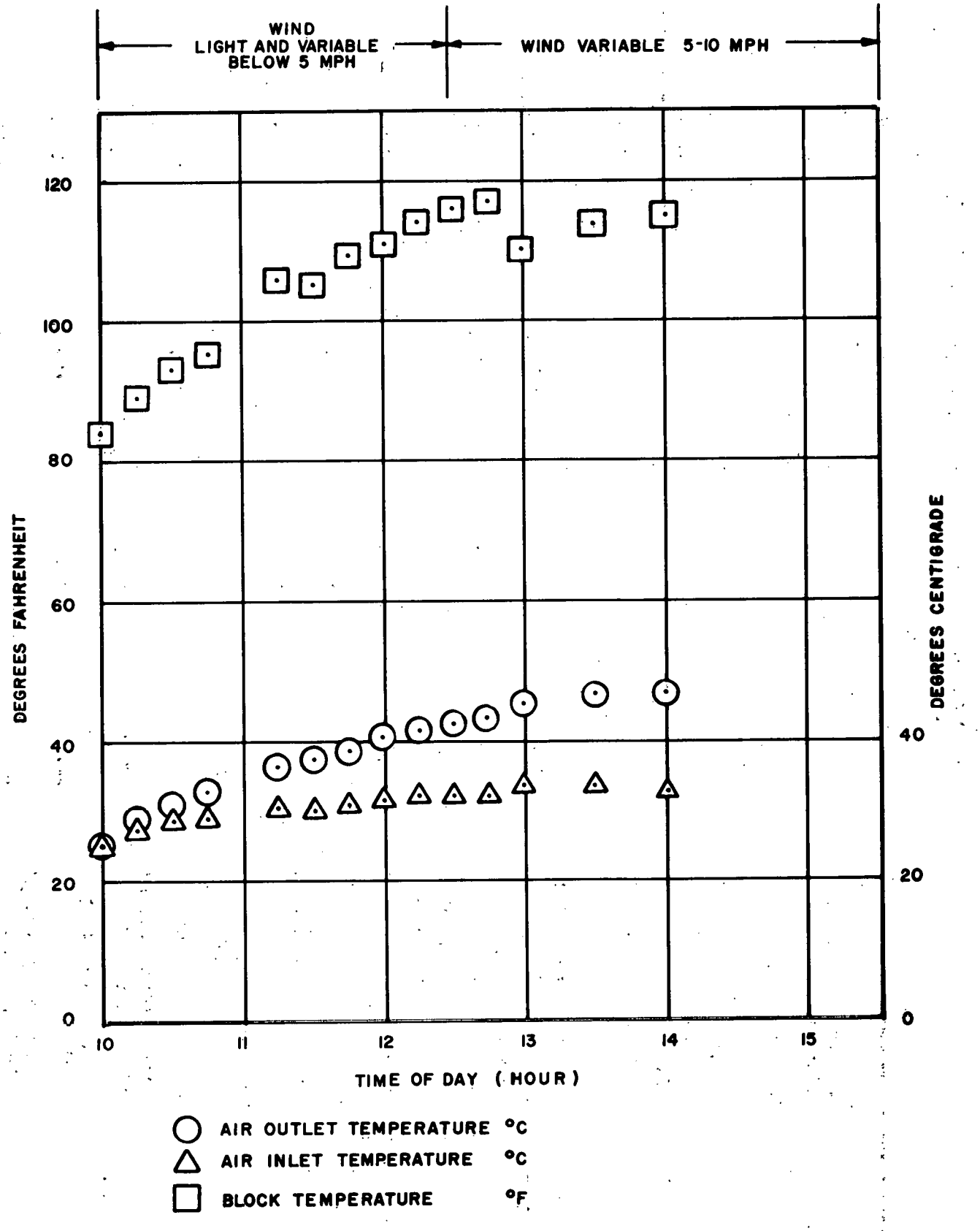

Figure 21. Air and block temperatures during the large block test on 6/1/78.

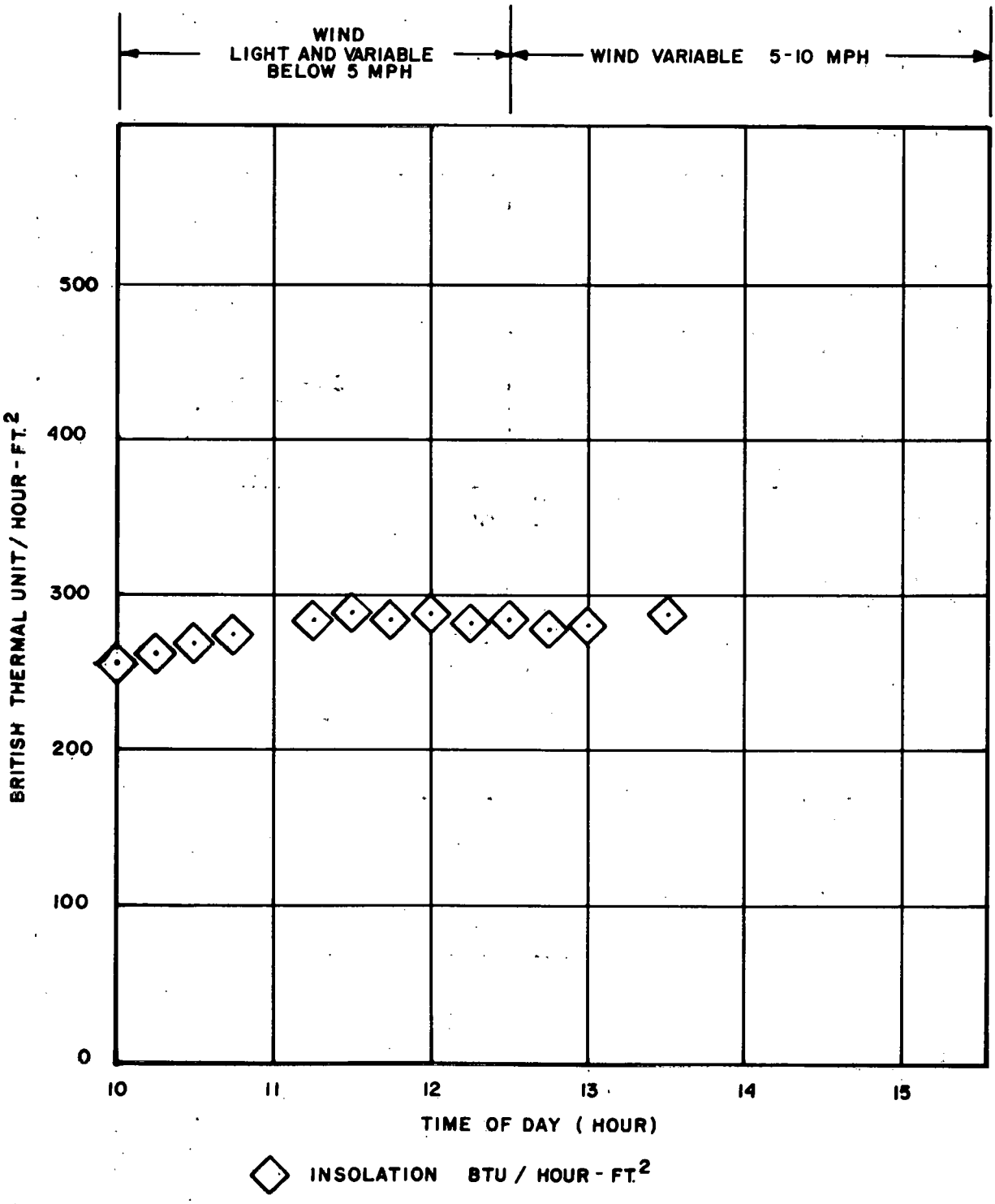

Figure 22. Insolation during the large block test on 6/1/78.

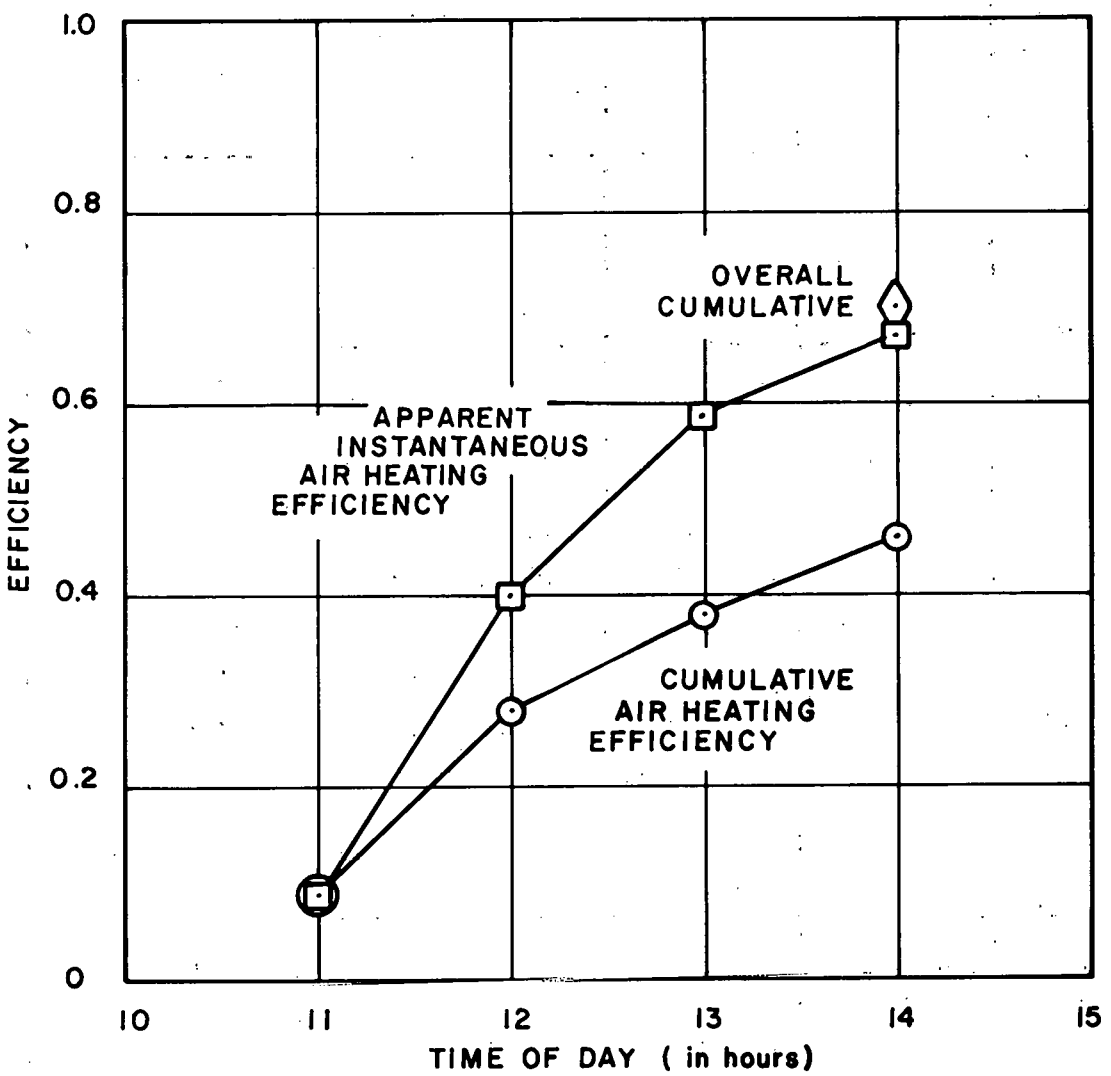

Figure 23. Efficiency of large 32" x 16" x 8" Payne open-face block; block was normal to sun during test. Double glazing of acrylic and polyester with a flow rate of 20.1 CFM. Block surface painted with Nextel black. Test was performed on 6/1/78.
Pressure Drop = 0.05 in. H_2O.

Table 5. Thermal performance of Cinder Block Wall.

	12:30-1:30	1:30-2:30	2:30-3:30
Average insolation (Btu/ft^2hr)	136	145	133
Average block temperature °F	113	120	125
Average ambient temperature °C (°F)	31.3(88.3)	31.5(88.7)	31.8(89.2)
Average outlet temperature °C (°F)	31.6(88.9)	34.9(94.8)	37.9(100.2)
ΔT (air) °C (°F)	0.3(0.6	3.4(6.1)	6.1(11.0)
Heat collected (air) (Btu/ft^2hr)	1.1	11.4	20.5
Average insulation loss (Btu/ft^2hr)	36.9	46.6	53.3
Total heat collected (Btu/ft^2hr) minus blower	37.9	58.0	73.8
Instant air efficiency	0.28	0.40	0.55
Cumulative insolation (Btu/ft^2)	136	281	414
Cumulative heat collected (Btu/ft^2)	37.9	95.9	169.7
Cumulative efficiency	0.23	0.34	0.41
Residual heat in block (Btu/ft^2) collected	54.5	46.8	39.0
Residual efficiency	0.68	0.72	0.85

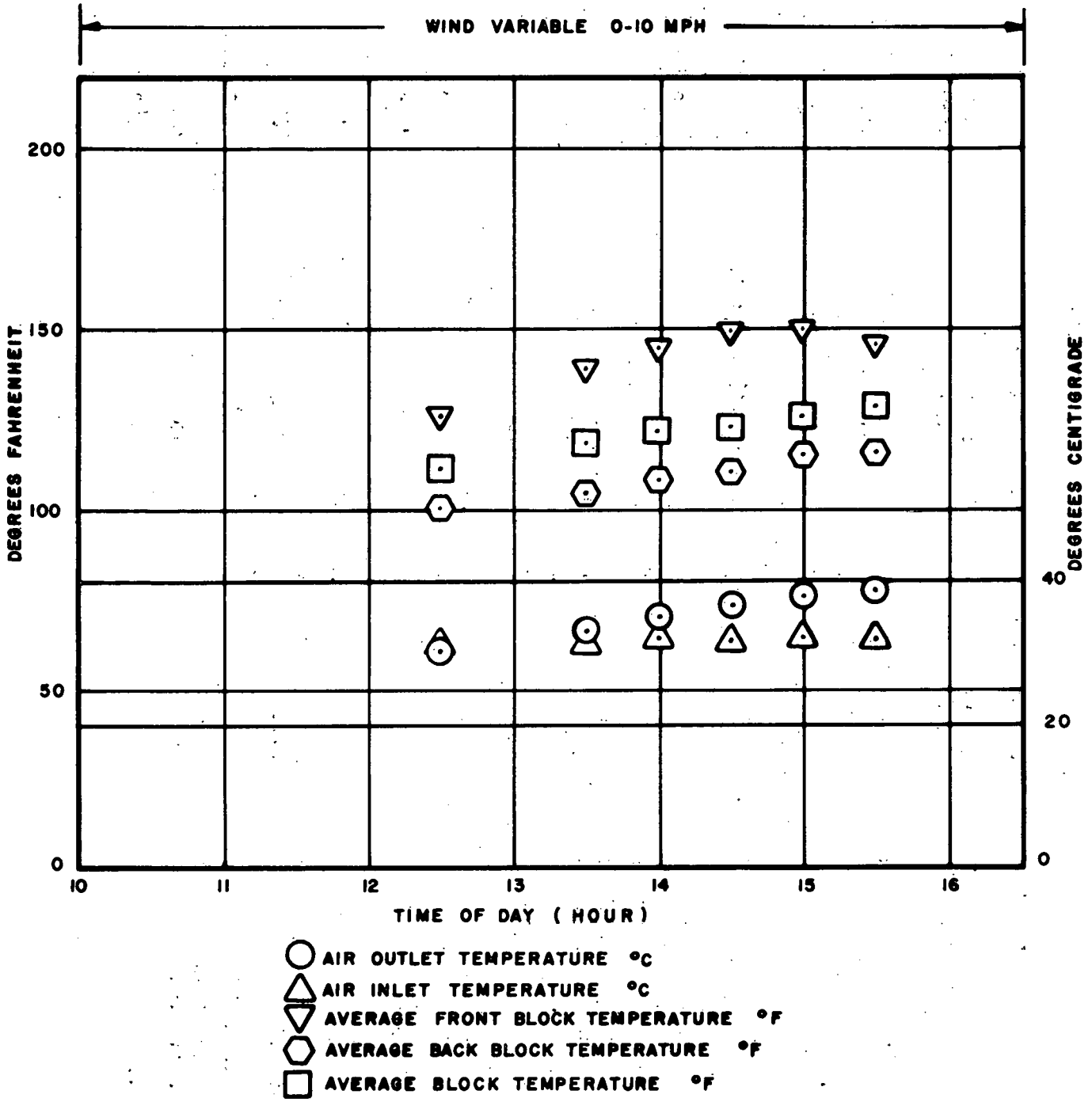

Figure 24. Air and block temperatures during the cinder block test on 6/29/78.

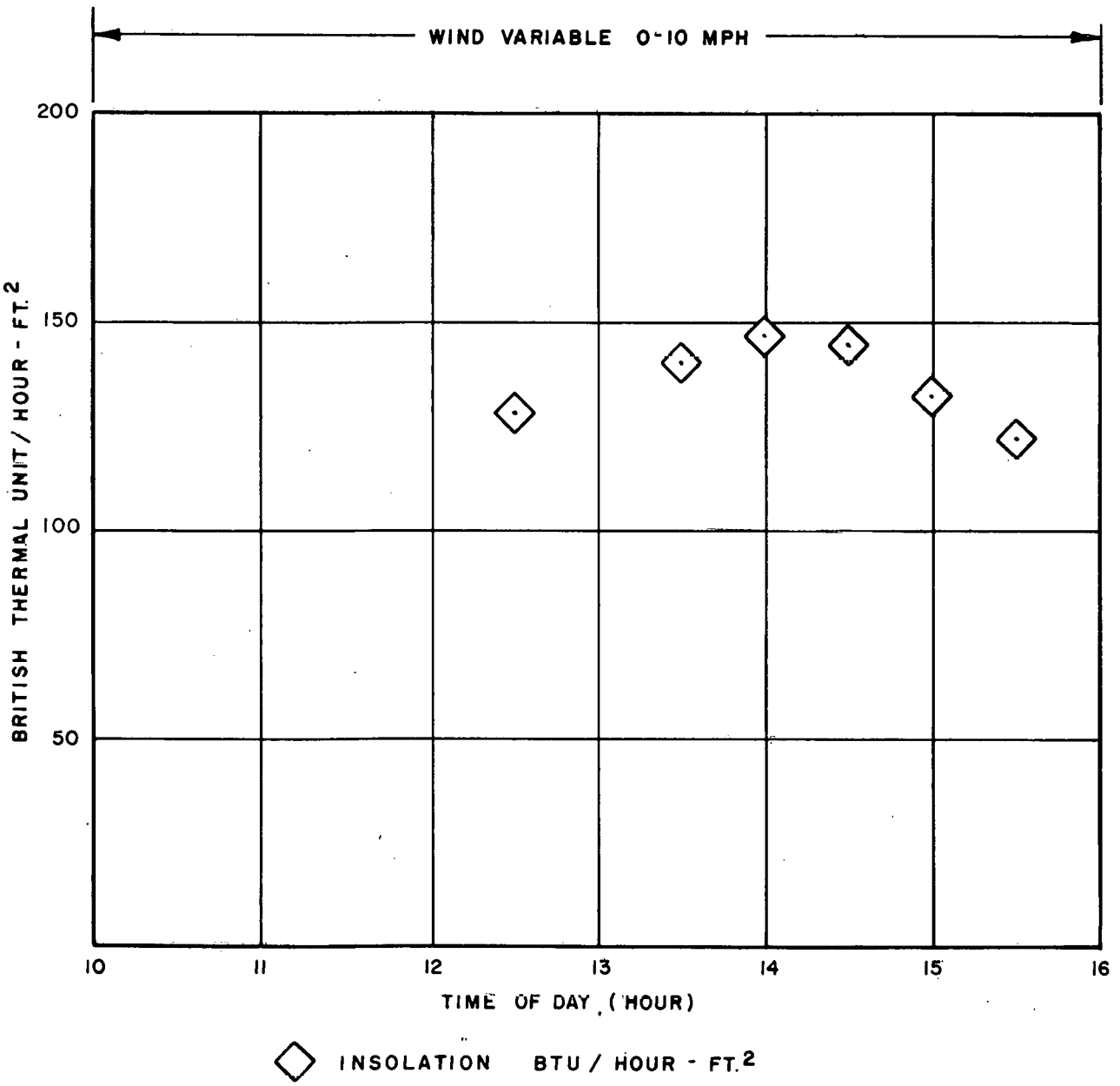

Figure 25. Insolation during the cinder block test on 6/29/78.

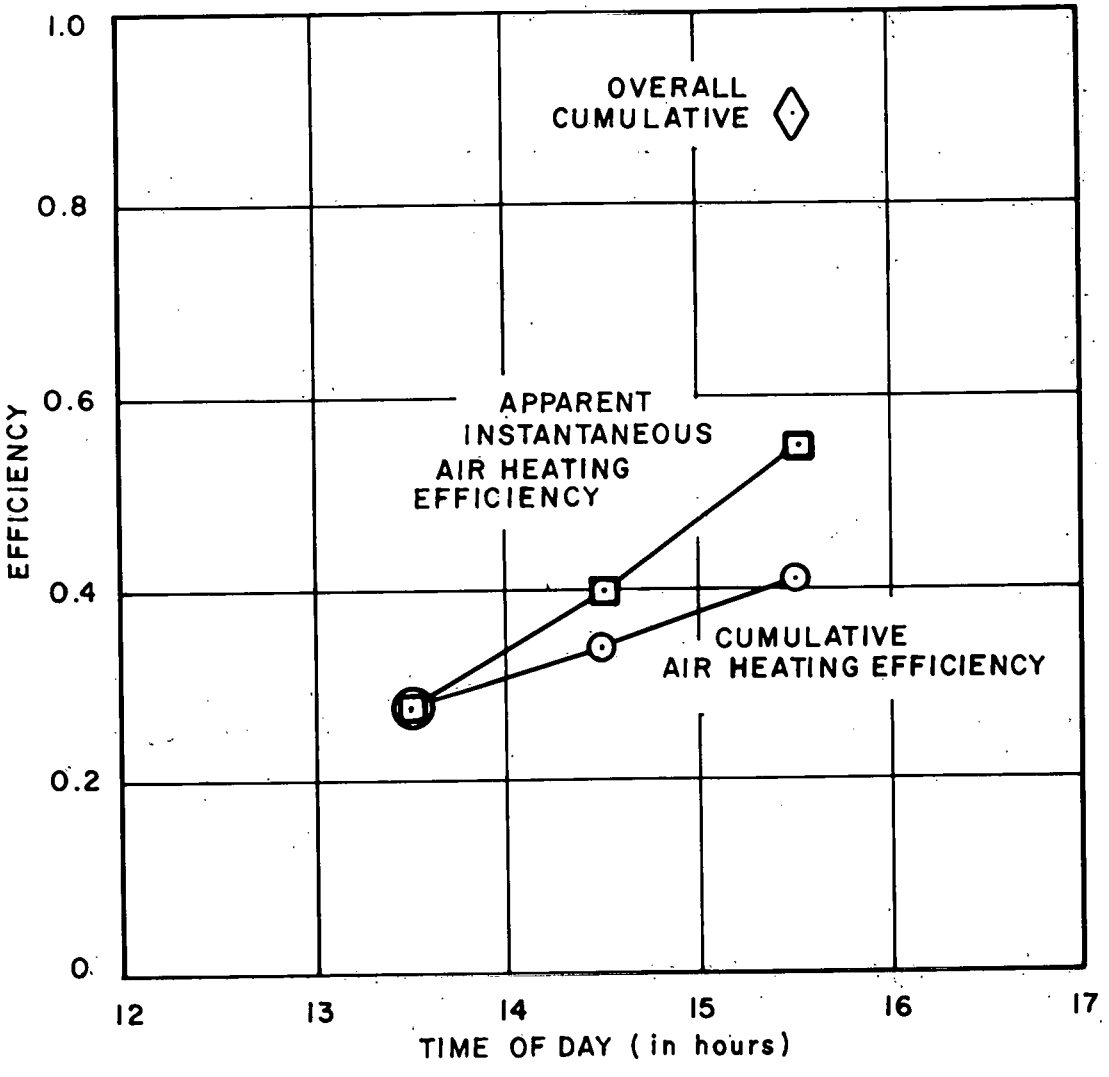

Figure 26. Efficiency of a conventional cinder block wall, aperture 13.8 ft^2, vertical and south-facing, on 6/29/78, at Annapolis, MD. Single glazing of acrylic with air passed through the block cores at 23.7 CFM. Block painted with Nextel black. Pressure drop = 0.03 in. H_2O.

Table 6. Thermal performance of Fluted Block on July 21, 1978

	11:00-12:00	12:00-1:00	1:00-2:00	2:00-3:00	3:00-4:00
Average insolation (Btu/ft^2hr)	102.0	119.4	123.0	111.2	89.8
Average block temperature °F	86.0	96.0	101.0	104.8	108.0
Average ambient temperature °C (°F)	28.6(83.5)	29.8(85.6)	31.4(88.5)	32.0(89.6)	32.2(89.6)
Average outlet temperature °C (°F)	29.7(85.5)	32.5(90.5)	35.0(95.0)	36.5(97.7)	36.4(97.5)
ΔT (air) °C (°F)	1.1(2.0)	2.7(4.9)	3.6(6.5)	4.5(8.1)	4.2(7.6)
Heat collected (air) (Btu/ft^2hr)	8.4	20.5	27.2	33.9	31.8
Average insulation loss (Btu/ft^2hr)	3.2	13.5	16.2	19.7	23.9
Total heat collected (Btu/ft^2hr) corrected for blower	10.7	33.1	42.5	52.7	54.8
Instant air efficiency	0.10	0.28	0.35	0.47	0.61
Cumulative insolation (Btu/ft^2)	102.0	221.4	344.4	455.6	545.4
Cumulative heat collected (Btu/ft^2)	10.7	43.8	86.3	139.0	193.8
Cumulative efficiency	0.10	0.20	0.25	0.31	0.36
Residual heat gain in block (Btu/ft^2hr)	66.7	41.8	19.1	29.0	0
Residual efficiency	0.76	0.63	0.50	0.73	0.61

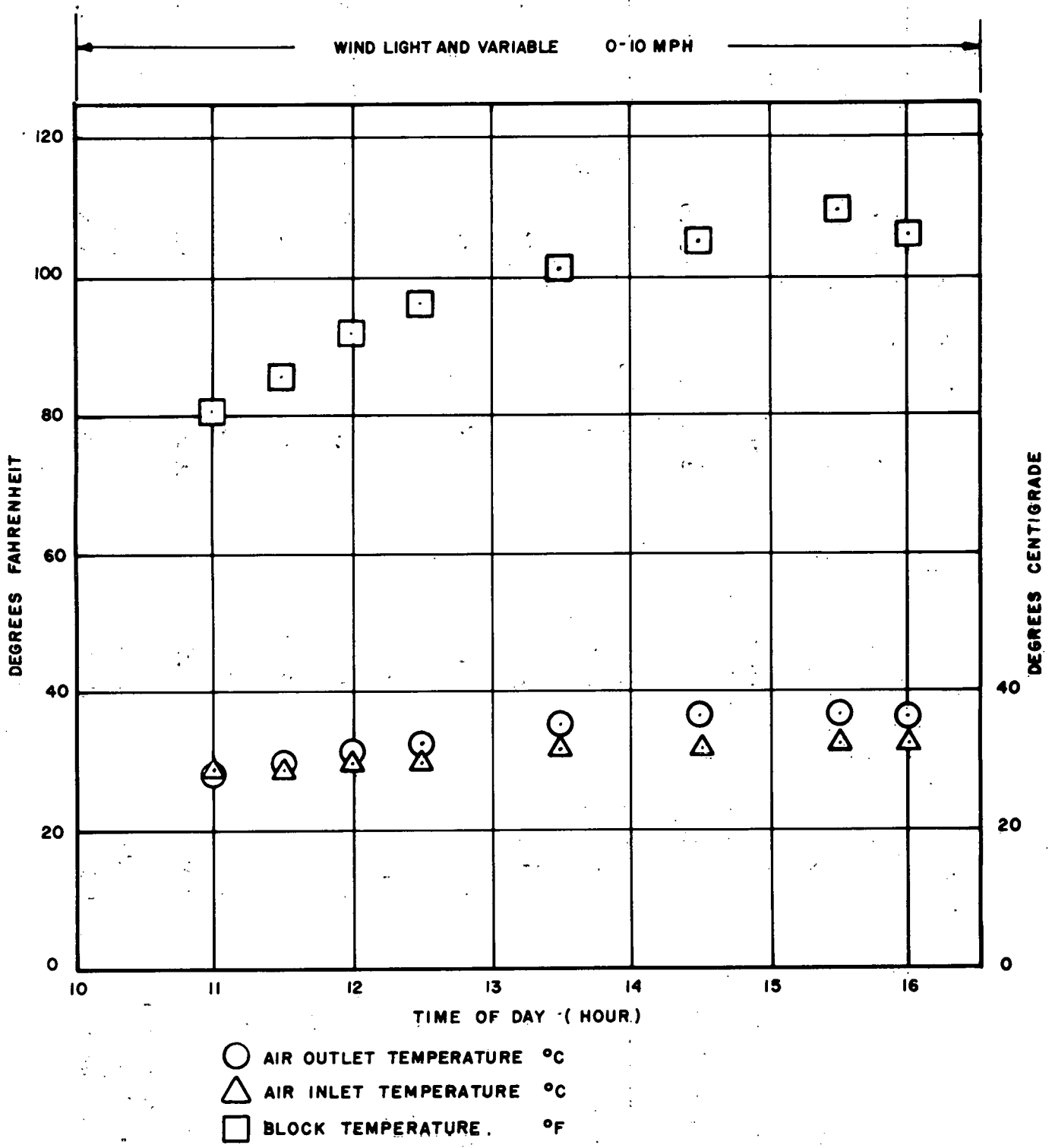

Figure 27. Air and block temperatures during the fluted block test on 7/21/78.

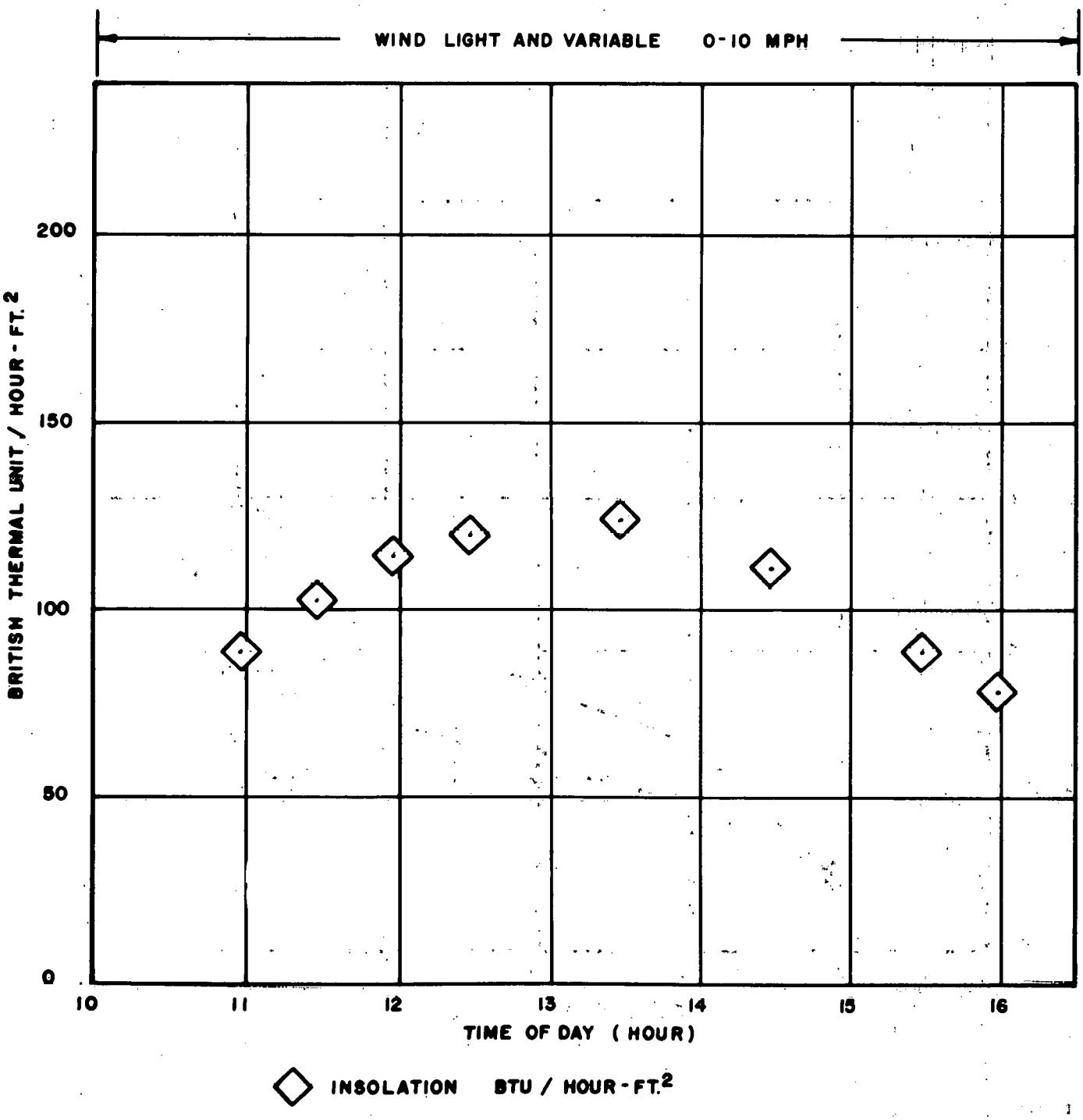

Figure 28. Insolation during the fluted block test on 7/21/78.

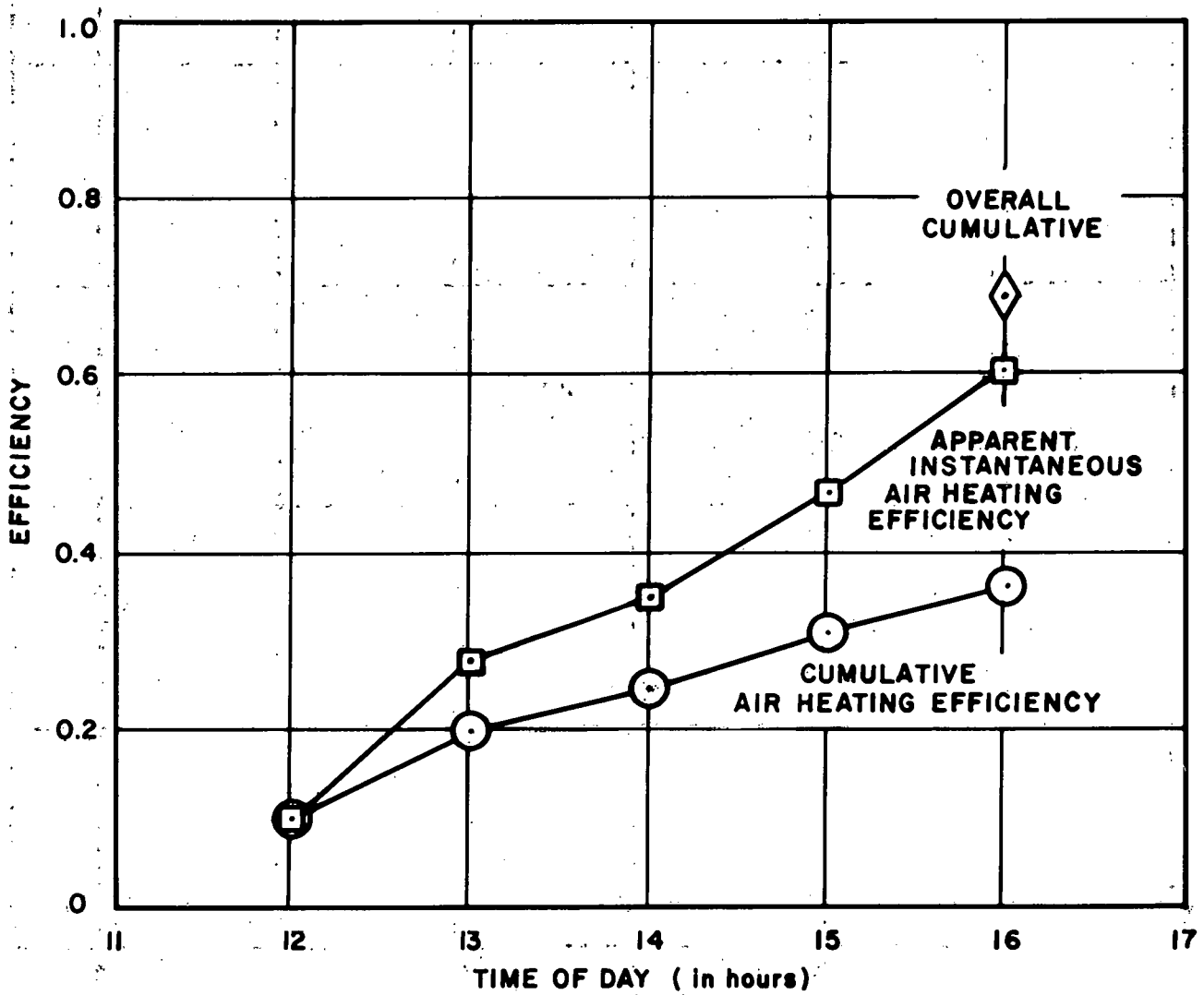

Figure 29. Fluted Block - aperture 15.7 ft^2, vertical and south-facing, on 7/21/78 at Annapolis, MD. Single acrylic glazing with an air flow of 60.5 CFM over the outer faces of "eight flute corduroy" blocks. Pressure Drop = 0.598 in. H_2O.

SOME THEORETICAL CONSIDERATIONS

A sealed collector has some form of wall between the incident solar radiation and the working fluid which carries away the heat from the wall. If the wall is very thick, or a poor conductor (or both) it's clear that collection efficiency will be reduced. The question is, how poor a conductor can the wall be before efficiency suffers significantly.

The simplest estimate occurs under equilibrium conditions. A typical result is given in Figure 30 for the following conditions:

Ambient temperature - 32°F
Collector fluid (air) inlet temperature - 60°F
Insolation - 200 Btu/ft^{2}hr.

As can be seen, a noticeable drop in efficiency occurs when the conductivity k/δ is less than 10 Btu/ft^{2}hr°F. So, based on these results we might say that, as a rule of thumb, a one inch thickness of concrete (or half an inch of cinderblock) is acceptable, but more is not. But such an analysis does not take into account the mass of the concrete which introduces a thermal inertia term into the equations, and greatly complicates the business of drawing simple conclusions. As just one example, the efficiency with which heat is absorbed by the outer surface of the concrete is susceptible to conventional analysis, and leads to the well known approximation

$$\eta = \eta_o + \eta_1 \frac{(T_{COL} - T_\infty)}{\Phi} + \ldots$$

We call this the "instantaneous efficiency."

But in the extreme case of a very thick wall, very little of the heat collected by this outer surface of the wall will have reached the working fluid by the end of the day. Most of the heat transfer from the inner surface of the concrete to the working fluid will take place during the night. So we have to define two other measures of performance:

$$\eta_A = \text{Apparent efficiency} = \frac{\text{Heat collected by day's end}}{\text{Total insolation}}$$

$$\eta_T = \text{Total efficiency} = \frac{\text{Heat collected in a 24 hour period}}{\text{Total insolation}}$$

In practice, after insolation has ceased for the day, a thick collector wall will not only loose heat to the working fluid, but will also radiate and convect heat away from it's front face. In the present analysis we have ignored this latter effect because, even without it, the physical picture is already quite complicated.

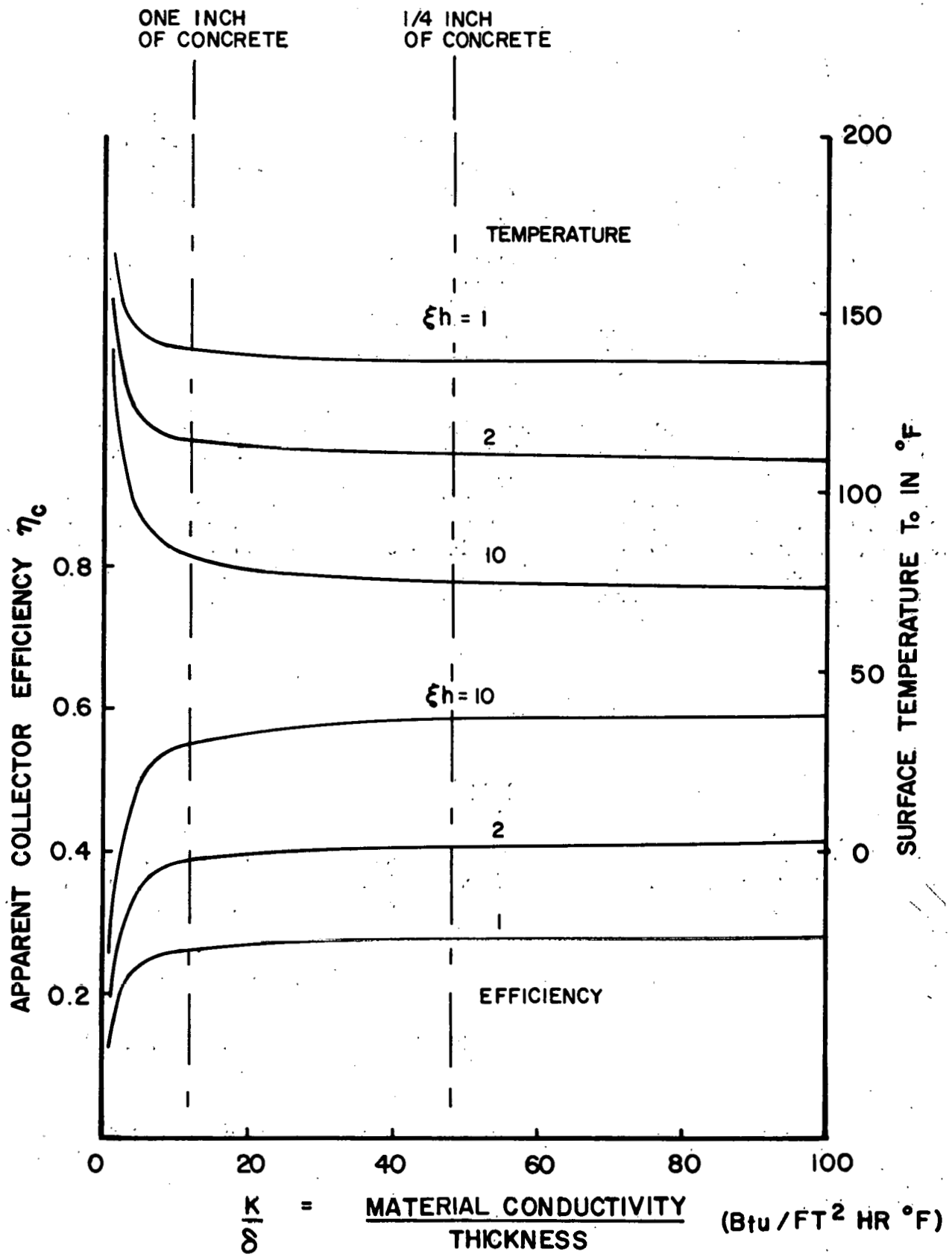

Figure 30. Effect of wall conductivity on collector performance for zero mass.
ξ = ratio of heat transfer surface to radiation area
h = heat transfer coefficient in Btu/ft^{2}hr°F
T_∞ = 32°F Φ = 200 Btu/ft^{2}hr
η_{co} = 0.8 η_1 = 0.8 T_F = 60°F

With these rather gross simplifications we obtain the sort of result shown in Figure 31. Here the assumed heat transfer coefficient (h) is rather low, the figure of 1 Btu/ft^{2}hr°F corresponding to a freely thermosiphoning collector. The temperature of the outer surface increases throughout the day, and is close to equilibrium after about six hours. Thus, for the first six hours, its instantaneous efficiency is higher than for a zero mass collector!* It is absorbing more heat than an ideal copper collector. Note also from Figure 31 that the initial temperature, at the start of insolation, has an an important effect upon performance. If the initial temperature is 20°F, over half an hour goes by before any heat is transferred to the working fluid.

At the end of the day, the collector wall has stored heat to transmit to the wall, and on the assumptions stated, it cools as indicated in Figure 32.

Figures 4 and 5 present more comprehensive data. In Figure 33 we have varied the heat transfer coefficient (h), and not surprisingly, find that efficiency improves with increasing values of h. In Figure 34 we see that increasing wall thickness has the same effect as reducing the heat transfer coefficient. Above a thickness of 3 inches, the wall does not even get up to equilibrium temperature during 8 hours of insolation. And more heat is transferred at night than during the day.

Total and apparent efficiencies for these cases are plotted in Figures 35 and 36. The sample zero mass efficiency of equations (5) and (6)† is here seen to be somewhat misleading in that it underestimates the total efficiency.

We conclude that there are probably no generalizations about the effectiveness of high mass and high resistance collectors expect that their total efficiency will not be much inferior to conventional collectors. If they can be built for significantly less (say less than half) the cost of "conventional" (i.e. high energy input) collectors, then their first cost amortization probably overrides all other considerations.

---

* Because its surface is cooler.

† Derived later in this section.

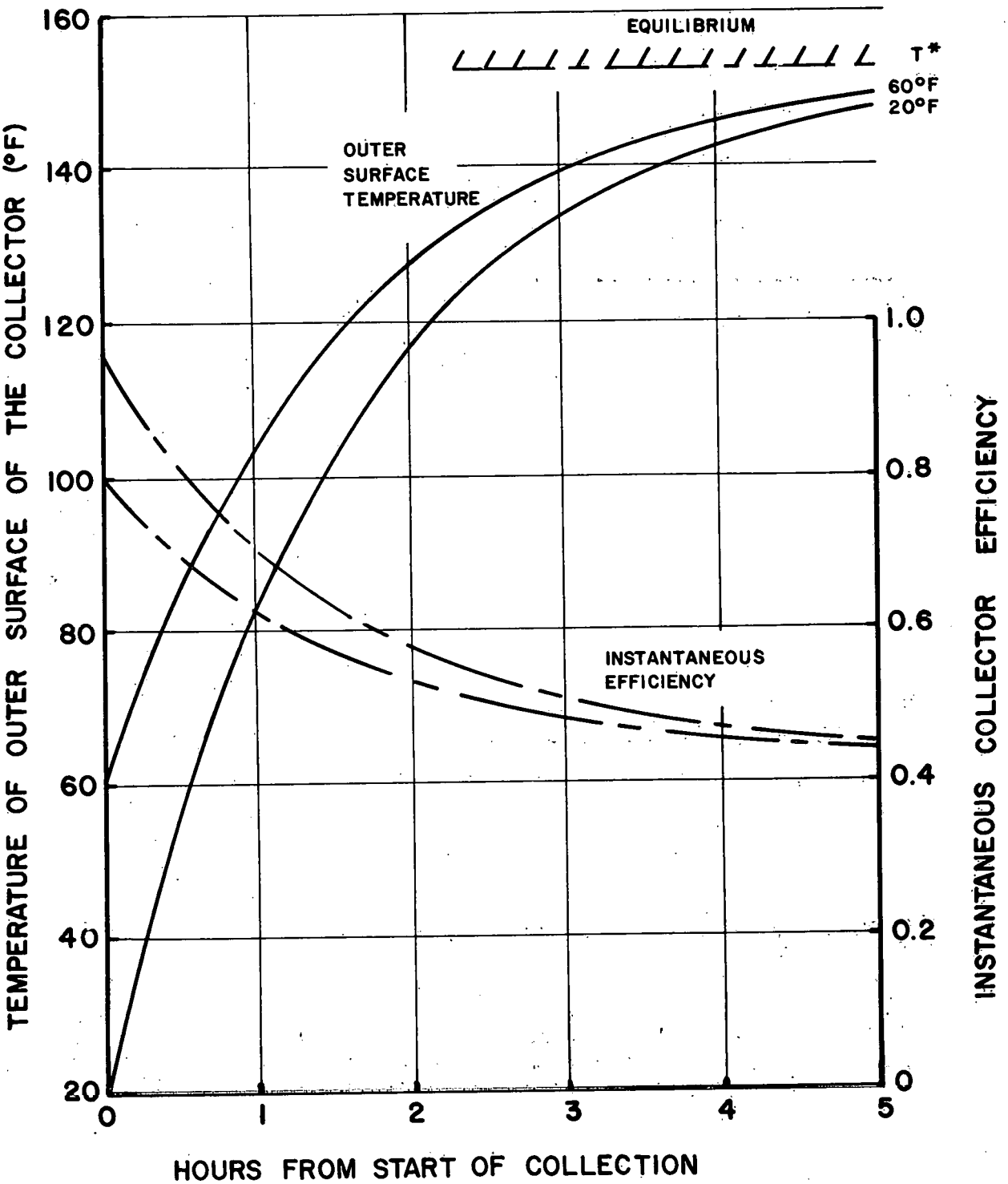

Figure 31. Collector surface temperature and instantaneous efficiency as a function of time. $T_\infty = 60°F$. $h = 1$ Btu/ft^{2}hr°F. One inch thick wall $\Phi = 200$ Btu/ft^{2}hr.

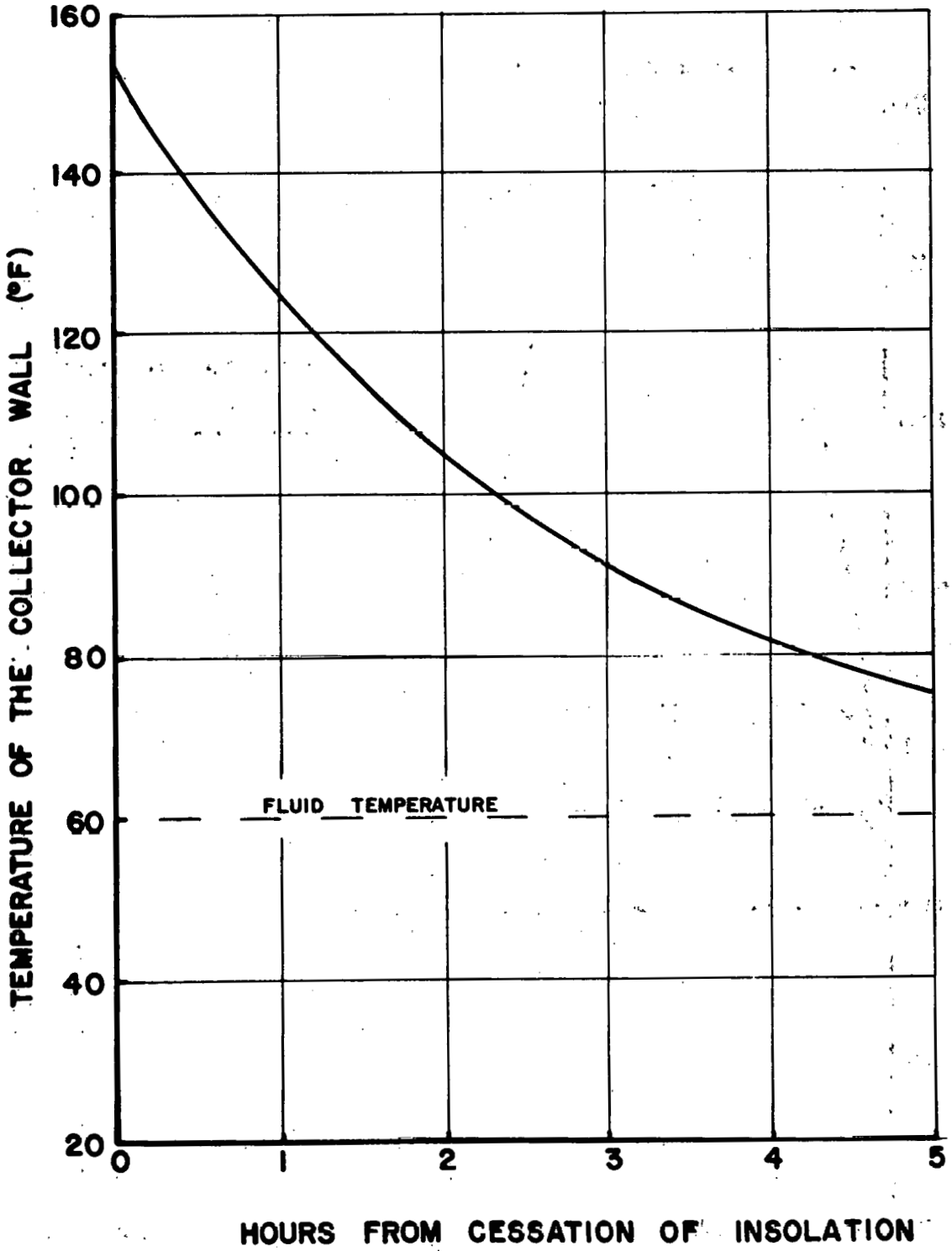

Figure 32. Collector wall temperature after cessation of insolation, assuming no losses (radiative or convective) to the outside.

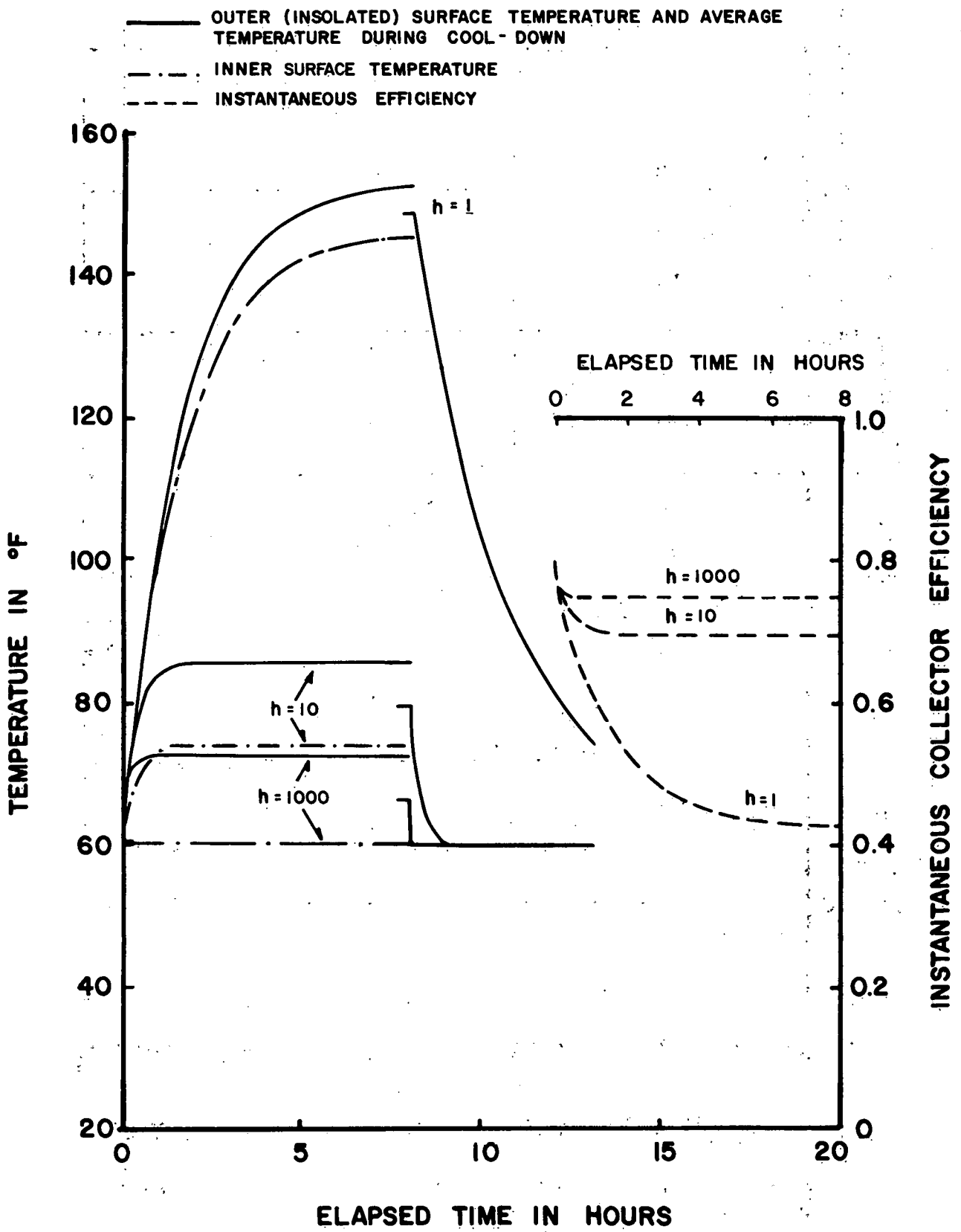

Figure 33. The effect of the fluid's heat transfer coefficient on collector warm-up and cooling down.
h = heat transfer coefficient in Btu/ft^{2}hr°F.
One inch wall thickness.

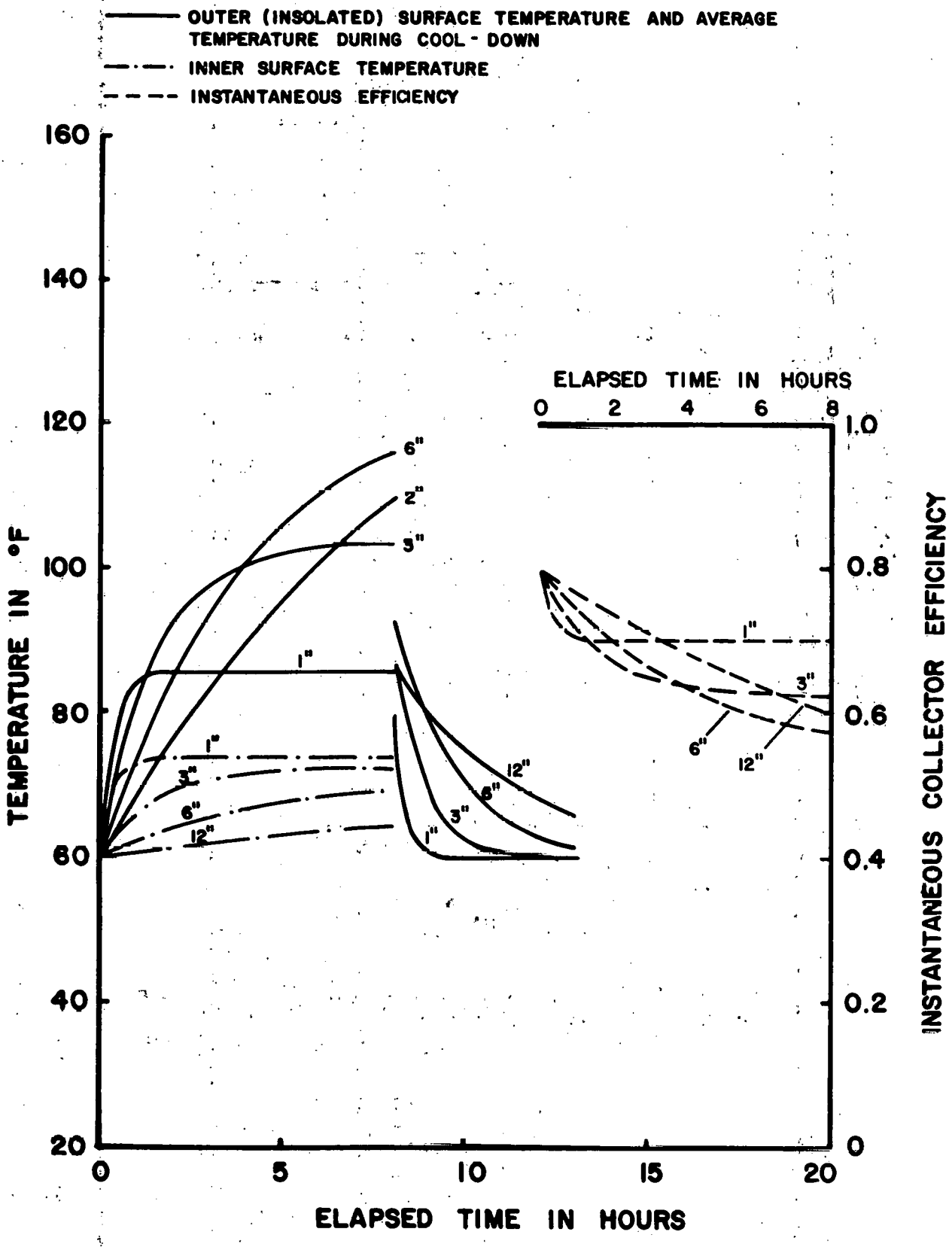

Figure 34. The effect of wall thickness on collector warm-up and cooling down. $h = 10$ Btu/ft^{2}hr°F

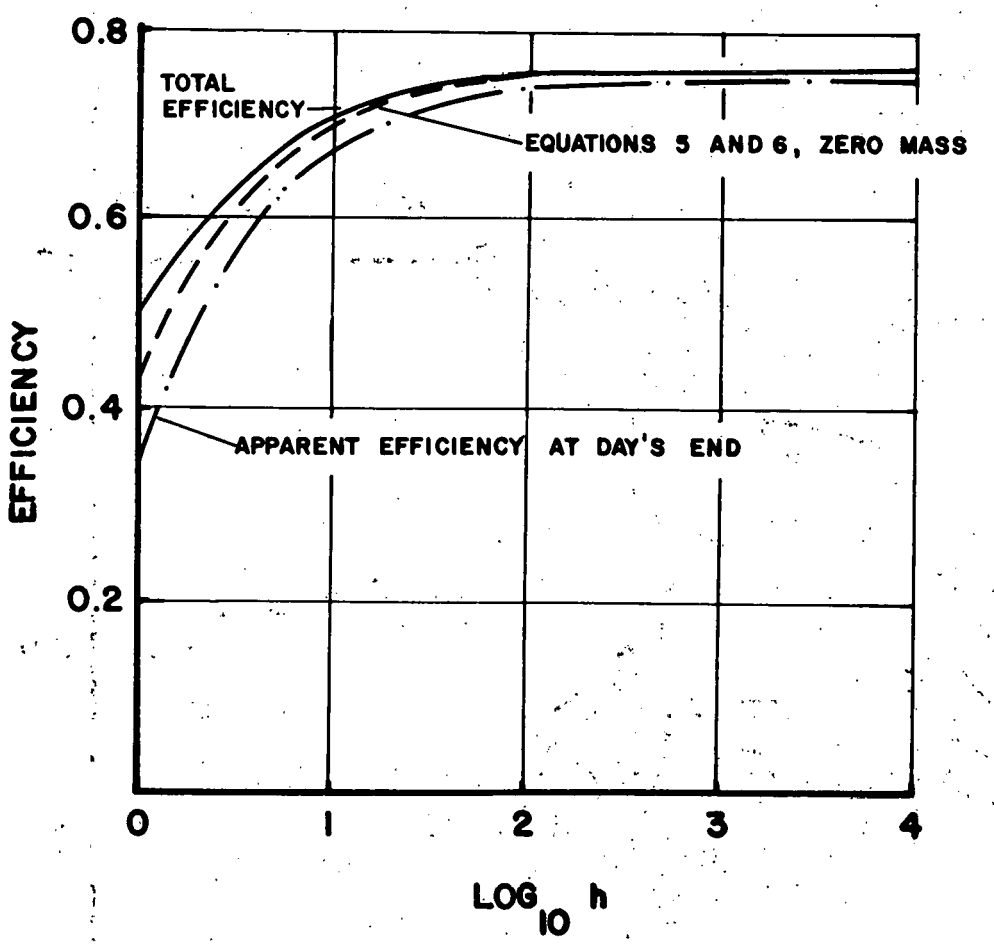

Figure 35. Effect of the heat transfer coefficient on overall efficiency of a one inch thick wall collector.

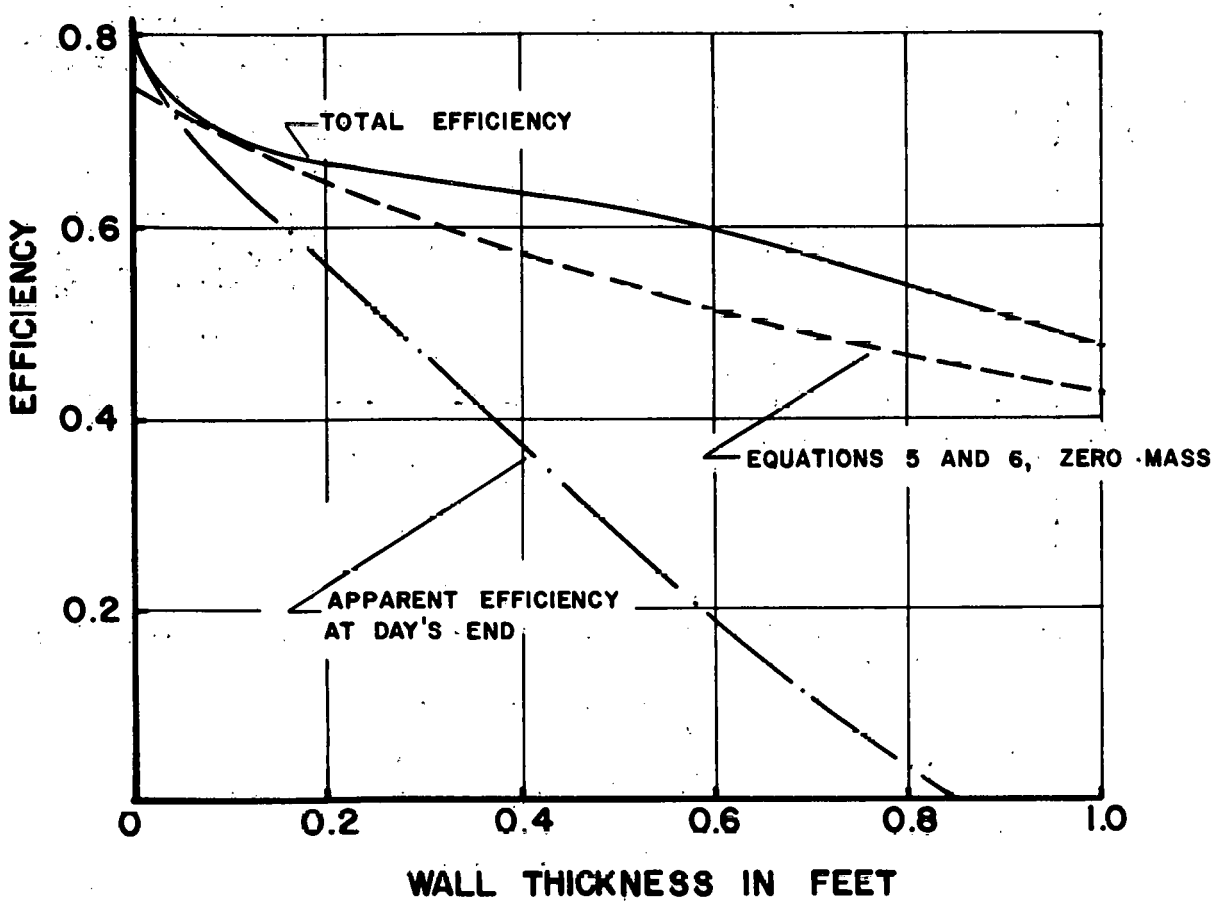

Figure 36. Effect of wall thickness on collector efficiency. h = 10 Btu/ft^{2}hr°F.

A collector with thermal resistance but no mass.

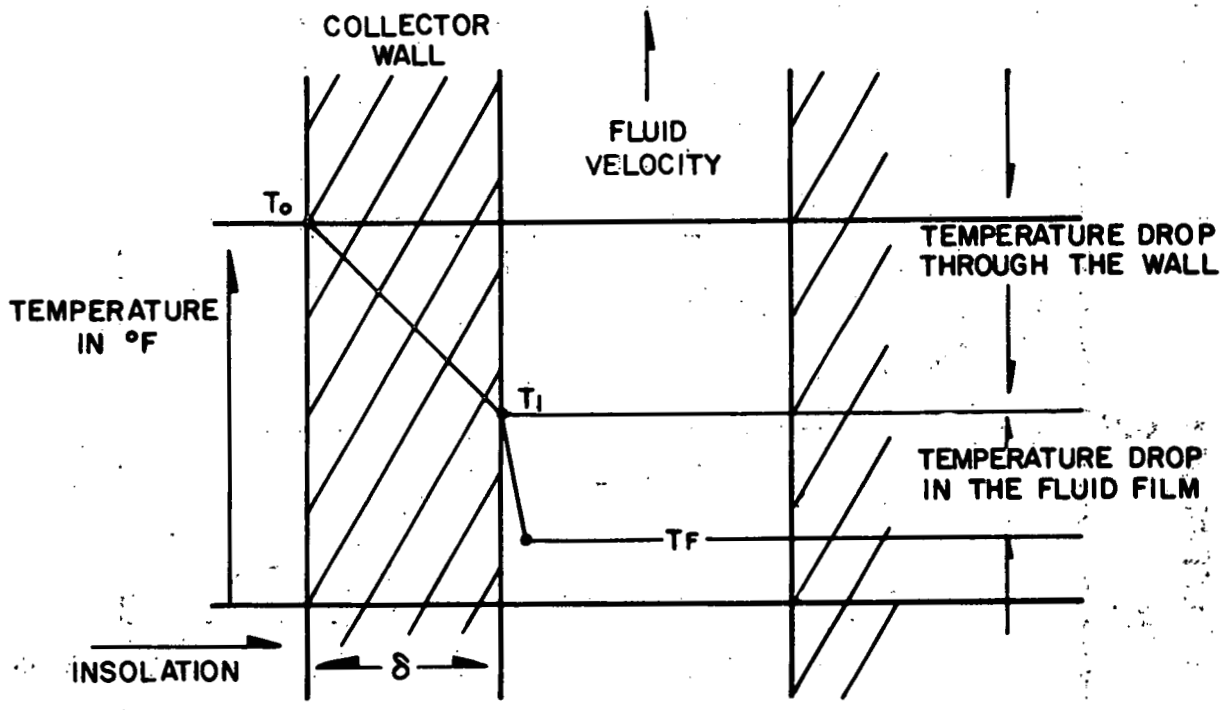

Assumed geometry

Let ξ = Internal heat transfer area per unit external area of the collector.
(= 1.0 if both surfaces are flat)
Φ = the incident insolation
η_c = collector efficiency based on heat collected at the front face.
k = material conductivity
δ = wall thickness
h = (film) heat transfer coefficient

At equilibrium:

$$\eta_c\Phi = \xi h(T_1 - T_F) = \frac{k}{\delta}(T_o - T_1) \tag{16}$$

$$\therefore\ T_o - T_1 = \frac{\eta_c\Phi\delta}{k} \tag{17}$$

$$\text{and } T_1 - T_F = \frac{\eta_c\Phi}{\xi h} \tag{18}$$

$$\therefore\quad T_o - T_F = \eta_c\Phi\left(\frac{\delta}{k} + \frac{1}{\xi h}\right) \tag{19}$$

If, as a first approximation we take

$$\eta_c = \eta_{co} - \frac{\eta_1(T_o - T_\infty)}{\Phi} \tag{20}$$

$$\text{So} \quad T_o = T_F + [\Phi\eta_{co} - \eta_1 (T_o - T_\infty)] \left(\frac{\delta}{k} + \frac{1}{\xi h} \right)$$

$$= \frac{T_F + (\Phi\eta_{co} + \eta_1 T_\infty) \left(\frac{\delta}{k} + \frac{1}{\xi h} \right)}{1 + \eta_1 \left(\frac{\delta}{k} + \frac{1}{\xi h} \right)} \tag{21}$$

Once T_o is computed, we can obtain η_c from equation (20)

The effect of thermal mass

In the Appendix, we show that for concrete walls of the order of 1 to 2 inches in thickness, the thermal gradient during heating or cooling is practically linear. Thus, we may write the transient heat balance equations as

$$\eta_c \Phi - \xi h (T_1 - T_F) = \frac{1}{2} \delta \rho g C_p \left(\frac{dT_o}{d\theta} + \frac{dT_1}{d\theta} \right) \tag{22}$$

Also, since

$$\xi h (T_1 - T_F) = \frac{k}{\delta} (T_o - T_1)$$

$$T_1 = \frac{\frac{k}{\delta} T_o + \xi h T_F}{\left(\xi h + \frac{k}{\delta} \right)} \tag{23}$$

Let $\alpha = \dfrac{\xi h}{\delta \rho g C_p}$

$$\eta_c = \eta_{co} - \eta_1 \frac{(T_o - T_\infty)}{\Phi}$$

$$\Psi_o = \frac{\eta_{co}\,\Phi}{\delta\rho g C_P} \qquad \Psi_1 = \frac{\eta_1}{\delta\rho g C_P}$$

$$\beta_1 = \frac{\frac{k}{\delta}}{\xi h + \frac{k}{\delta}} \qquad \beta_2 = \frac{\xi h}{\xi h + \frac{k}{\delta}}$$

Thus equations (22) and (23) become

$$\Psi_o - \Psi_1 (T_o - T_\infty) - \alpha(T_1 - T_F) = \frac{1}{2}\frac{dT_o}{d\theta} + \frac{1}{2}\frac{dT_1}{d\theta} \tag{24}$$

$$T_1 = \beta_1 T_o + \beta_2 T_F \tag{25}$$

$$\frac{dT_1}{d\theta} = \beta_1 \frac{dT_o}{d\theta} \tag{26}$$

Substituting (25) and (26) for T_1 and $\frac{dT_1}{d\theta}$ into equation (24)

$$\frac{1}{2}(1 + \beta_1)\frac{dT_o}{d\theta} + (\Psi_1 + \alpha\beta_1)T_o = \Psi_o + \Psi_1 T_\infty + \alpha(1 - \beta_2)T_F \tag{27}$$

Let $P = \frac{2(\Psi_1 + \alpha\beta_1)}{(1 + \beta_1)}$

$$Q_1 = \frac{2(\Psi_o + \Psi_1 T_\infty)}{(1 + \beta_1)}$$

$$Q_2 = \frac{2\alpha(1 - \beta_2)}{(1 + \beta_1)}$$

$$\text{Thus } \frac{dT_o}{d\theta} + PT_o = Q_1 + Q_2T_F \tag{28}$$

$$\text{and } T_o = e^{-P\theta}\left[\int e^{P\theta}[Q_1 + Q_2T_F]d\theta + C \right] \tag{29}$$

For the simplest case of constant T_F

$$T_o = \frac{[Q_1 + Q_2T_F]}{P} + Ce^{-P\theta}$$

when $\theta = 0$, $T = T^*$ say

$$\therefore C = T^* - \frac{[Q_1 + Q_2T_F]}{P}$$

$$\therefore T_o = T^*e^{-P\theta} + \frac{[Q_1 + Q_2T_F]}{P}(1 - e^{-P\theta}) \tag{30}$$

Note that as $\theta \to \infty$

$$T_o \to \frac{Q_1 + Q_2T_F}{P} = \frac{\Psi_o + \Psi_1T_\infty + \alpha(1 - \beta_2)T_F}{\Psi_1 + \alpha\beta_1} \tag{31}$$

Which reduces to equation (21)

$$\text{i.e. } T_o = T^*e^{-P\theta} + T_{o_{EQUIB}}(1 - e^{-P\theta}) \tag{32}$$

For average concrete

$\rho g = 145$ lb/ft^3
$Cp = 0.23$ Btu/lb°F
$\delta = 1/12$ ft
$k = 1$ Btu/ft.hr.°F

Also taking $\eta_{co} = \eta_1 = 0.8, \quad \xi = 1$

$h = 1$ Btu/ft^{2}hr°F
$\Phi = 200$ Btu/ft^{2}hr
$T_\infty = 60°F$
$T^* = 20°F$

We have $$\alpha = \frac{1 \times 1}{\frac{1}{12} \times 145 \times 0.23} = 0.3598$$

$$\Psi_o = \frac{0.8 \times 200}{\frac{1}{12} \times 145 \times 0.23} = 57.571$$

$$\Psi_1 = \frac{0.8}{\frac{1}{12} \times 145 \times 0.23} = 0.28786$$

$$\beta_1 = \frac{12}{1 + 12} = 0.92308$$

$$\beta_2 = \frac{1}{1 + 12} = .076923$$

$$P = \frac{2(0.28786 + 0.3598 \times 0.92308)}{1.92308} = 0.64478 \text{ hr}^{-1}$$

$$Q_1 = \frac{2(57.571 + 0.28786 \times 60)}{1.92308} = 77.8362$$

$$Q_2 = \frac{2 \times 0.3598(1 - .076923)}{1.92308} = 0.34541$$

$$\therefore T_o^* = 20e^{-0.64478\theta} + 152.86(1 - e^{-0.64478\theta})$$

This is plotted in Figure 31.

It is now necessary to compute the fall in temperature after the insolation has ceased. Because of the small thermal gradient in the wall, it's sufficient to take the wall temperature as uniform across its thickness, initially at the elevated maximum value T_M. Then if there is no radiative or other loss from the front face

$$\xi h(T_1 - T_F) = \delta\rho g C_P \frac{dT_1}{d\theta}$$

$$\text{or } \frac{dT_1}{d\theta} + \alpha T_1 = \alpha T_F \tag{33}$$

$$\text{so } T_1 = e^{-\alpha\theta}\left[\int e^{\alpha\theta}\alpha T_F d\theta + C\right]$$

$$= T_F + Ce^{-\alpha\theta}$$

$$\text{when } \theta = 0,\ T_1 = T_M \text{ so } C = T_M - T_F$$

$$\therefore T_1 = T_F + (T_M - T_F)e^{-\alpha\theta} \tag{34}$$

This is plotted in Figure 32 for the previous example, on the assumption that insolation continued at a constant level for eight hours, and was then cut off. It's noteworthy that considerable heat is transferred for several hours after the cessation of insolation.

Total heat transference

If insolation is constant for a period θ_s the heat transferred to the working fluid during this time is

$$\Delta Q_s = \int_0^{\theta s} \xi h(T_1 - T_F)d\theta$$

$$= \xi h \int_0^{\theta s} [\beta_1 T_o + \beta_2 T_F - T_F]d\theta$$

$$= \xi h \int_0^{\theta_s} [\beta_1 T^* e^{-P\theta} + \beta_1\left[\frac{Q_1 + Q_2 T_F}{P}\right](1 - e^{-P\theta}) - T_F(1 - \beta_1)]d\theta$$

$$= \xi h\left\{\frac{\beta_1 T^*}{P}(1 - e^{-P\theta_s}) + \beta_1\left[\frac{Q_1 + Q_2 T_F}{P}\right]\left[\theta_s - \frac{(1 - e^{-P\theta_s})}{P}\right] - T_F(1 - \beta_2)\theta_s\right\} \tag{35}$$

The heat which can potentially be transferred after time θ_s is

$$\Delta Q_D = \xi h \int_o^\infty (T_1 - T_F) d\theta$$

$$= \xi h \int_o^\infty [T_F + (T_M - T_F) e^{-\alpha\theta} - T_F] \, d\theta$$

$$= \frac{\xi h}{\alpha} (T_M - T_F) = \delta \rho g C_p (T_M - T_F) \qquad (36)$$

Where T_M is the maximum value of T_1. For relatively thin walls

$$T_1 = \frac{(T_{oM} + T_{1M})}{2}$$

where M denotes the value when the insolation ceases.

CONCLUSIONS AND RECOMMENDATIONS

1. The tests carried out in this program were fairly limited in scope. With that reservation, they indicate that concrete block air heaters are not significantly less efficient than more sophisticated metallic and plastic solar collectors. This agrees with our theoretical analyses.

2. The specially designed blocks were not significantly more efficient than "off the shelf" designs already available. But the sun was nearing its highest point in the sky during the tests, and there are theoretical grounds for anticipating a different result with low winter sun elevations.

3. South-facing concrete block walls can be effectively used as solar collectors for a cost roughly equal to their glazing cost; say less than one dollar per square foot.

4. Lengthier and more elaborate tests with a large scale wall should be carried out.

5. More research should be conducted with collectors made from low energy of formation materials such as concrete and ceramic. Present indications are that they can recover their "fossil fuel investment" in less than one heating season, whereas some metallic collectors may never recover their investment.

APPENDIX

HEAT FLOW THROUGH A CONCRETE WALL

Let
a = thermal diffusivity = $k/C_p\rho g$
C_p = specific heat of the material
ρg = specific weight of the material
k = the material's conductivity
η = $x/2\sqrt{a\theta}$
x = distance into the mass from its outside edge
ℓ = thickness of the mass
$\hat{x}$ = x/ℓ
q = heat flux at $x = \ell$
T = temperature at some location x in the mass
T_o = initial slab temperature

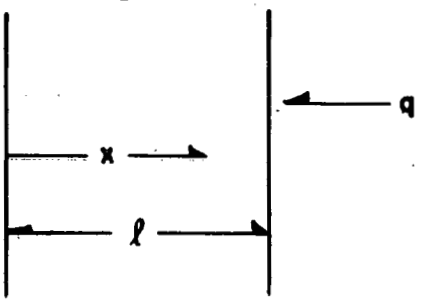

The inner surface is adiabatic. For this case Carslaw and Jaeger[8] give

$$\frac{T - T_o}{q} = \frac{2\sqrt{a\theta}}{k} \sum_{u=0}^{\infty} \left\{ \text{ierfc} \frac{(2u+1)\ell - x}{2\sqrt{a\theta}} + \text{ierfc} \frac{(2u+1)\ell + x}{2\sqrt{a\theta}} \right\}$$

This has been solved, in Figures A1 and A2 for typical concrete block wall thickness, where it's clear that the transient heat flow effects are unimportant. So we can write the heat balance equation as

$$\rho g \ell C_p (T - T_o) = q\theta = h(T_F - T)\theta$$

where h is the heat transfer (film) coefficient
T_F is the fluid temperature

For convenience, values of h are given in Figure A3. A fair approximation is seen to be $h = v/3$, where the flow speed v is in ft/sec.

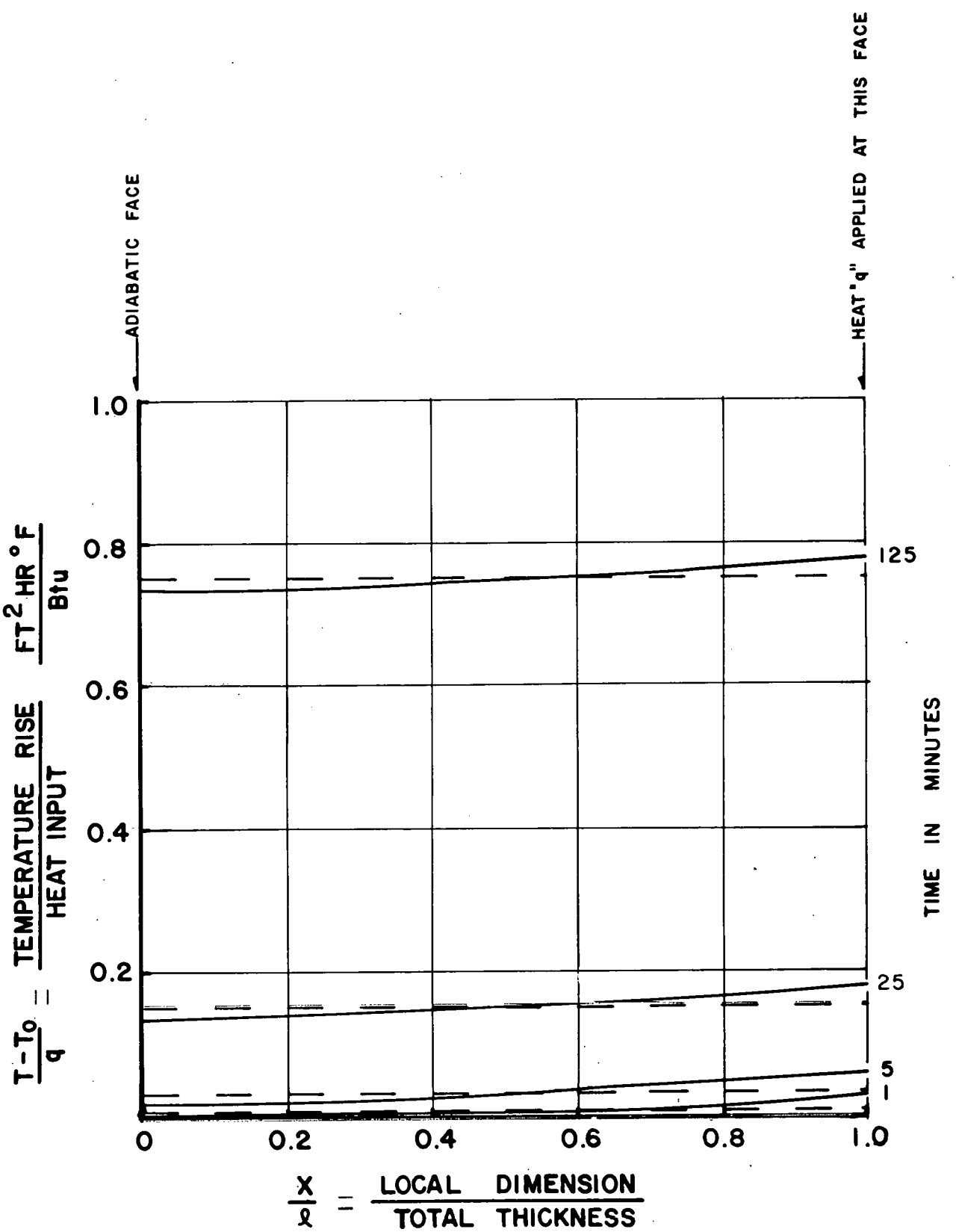

Figure A1. Temperature rise in a one inch thick concrete slab. The dotted horizontal lines are

$$\frac{T - T_0}{q} = \frac{\theta}{\rho g C_p \ell}$$

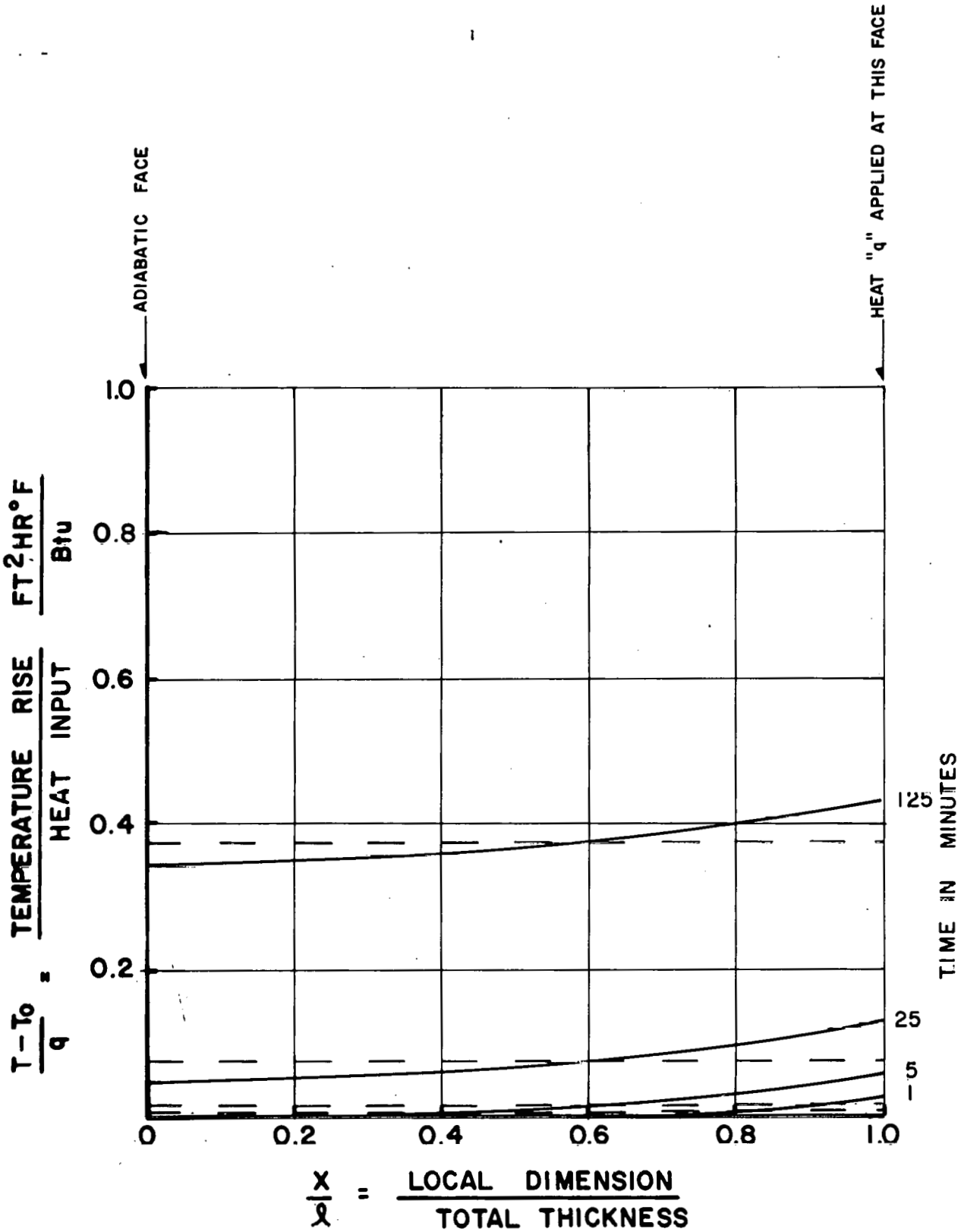

Figure A2. Temperature rise in a two inch thick concrete slab. The dashed horizontal lines are:

$$\frac{T - T_0}{q} = \frac{\theta}{\rho g C_p \ell}$$

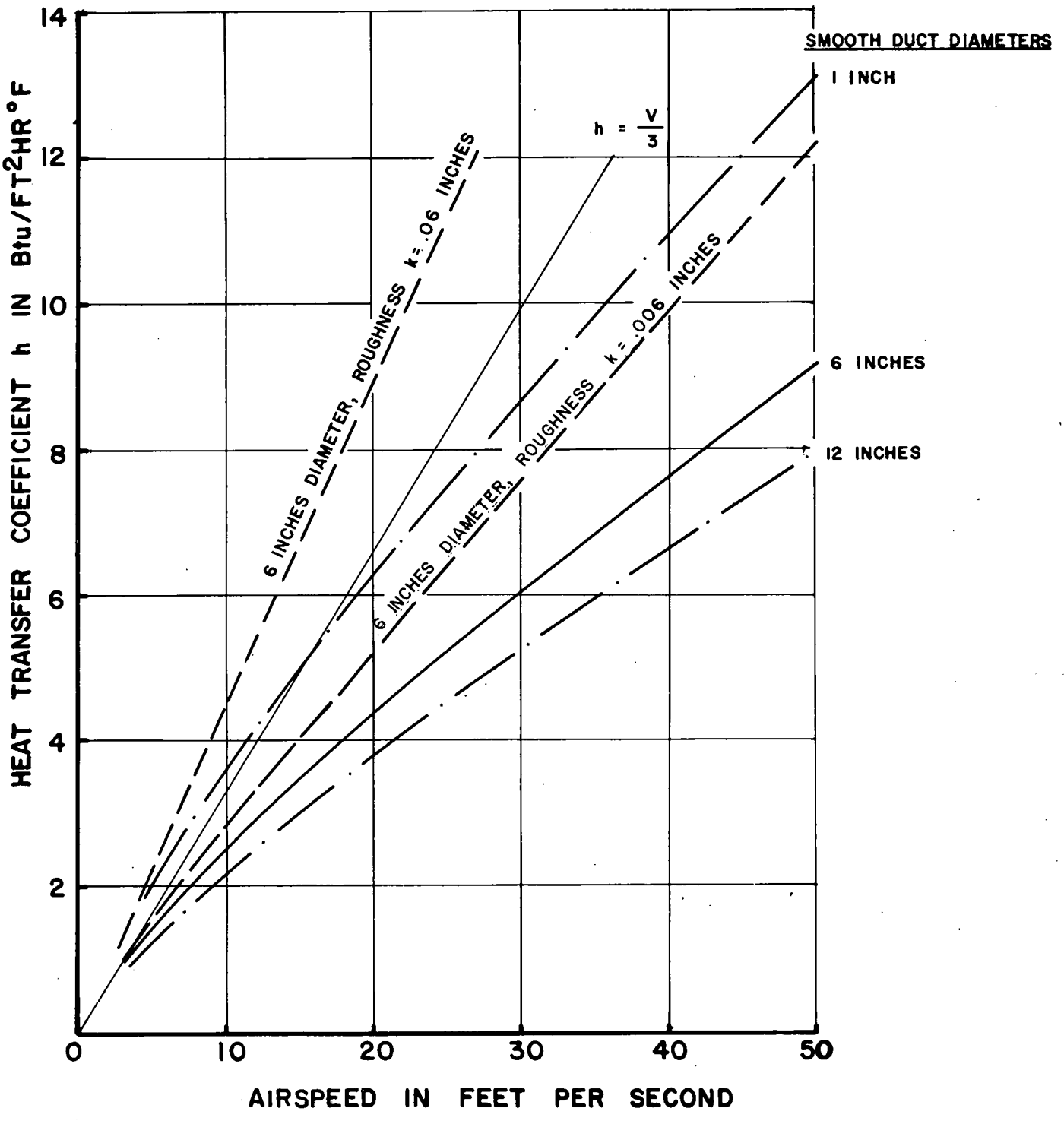

Figure A3. Heat transfer coefficient solid to air.

REFERENCES

1. Payne, P.R. "Thermal Equilibrium of a Pool or Lake." Payne, Inc. Working Paper No. 220-1, December 1977.

2. Payne, P.R. "Transfer of Heat from a Vertical Plate to Convective Air Flow." Payne, Inc. Working Paper No. 220-2, January 1978.

3. Payne, P.R. "The One Dimensional Performance of a Collector Having High Thermal Resistance and Inertia." Payne, Inc. Working Paper No. 220-5, March 1978.

4. Payne, P.R. "The Relationship Between Surface Area and Mass in a Heat Storage Mass." Payne, Inc. Working Paper No. 220-6, March 1978.

5. Payne, P.R. "A Note on the Fluid Dynamics of a Trickle Collector." Payne, Inc. Working Paper No. 220-8, April 1979.

6. Payne, P.R. "A Note on Heat Loss Through Glazing." Payne, Inc. Working Paper No. 220-9, April 1979.

7. Schlichting, H. Boundary Layer Theory, 4th edition. New York: McGraw-Hill Book Co., Inc., 1960.

8. Carslaw, H.S. and Jaeger, J.C. Conduction of Heat in Solids, Second Edition. New York: Oxford University Press, 1959.

☆U.S. GOVERNMENT PRINTING OFFICE: 1981-740-145/1330